

1 **TITLE**

2 **Downregulation of *Let-7* miRNA promotes Tc17 differentiation and emphysema via de-**  
3 **repression of RORyt**

4

5 **AUTHORS**

6 Phillip A. Erice<sup>1,2</sup>, Xinyan Huang<sup>2,6</sup>, Matthew J. Seasock<sup>1,2</sup>, Matthew J. Robertson<sup>3</sup>, Hui-Ying,  
7 Tung<sup>4</sup>, Melissa A. Perez-Negron<sup>2</sup>, Shivani L. Lotlikar<sup>2</sup>, David B Corry<sup>2,4,6</sup>, Farrah Kheradmand<sup>4,5,6</sup>,  
8 Antony Rodriguez<sup>2,6\*</sup>

9

10 <sup>1</sup>Immunology Graduate Program, Baylor College of Medicine, Houston, TX, 77030.

11 <sup>2</sup>Department of Medicine, Immunology & Allergy Rheumatology, Baylor College of Medicine  
12 Houston TX, 77030.

13 <sup>3</sup>Dan Duncan Comprehensive Cancer Center, Baylor College of Medicine Houston, TX, 77030.

14 <sup>4</sup>Department of Pathology and Immunology, Baylor College of Medicine Houston, TX, 77030.

15 <sup>5</sup>Department of Medicine, Section of Pulmonary and Critical Care, Baylor College of Medicine.  
16 Houston, TX, 77030.

17 <sup>6</sup>Center for Translational Research on Inflammatory Diseases, Michael E. DeBakey, Baylor  
18 College of Medicine, Houston, TX, 77030.

19 <sup>7</sup>Current address, Department of Pulmonary and Critical Care Medicine, The First Affiliated  
20 Hospital of Sun Yat-sen University. Guangzhou, Guangdong Province, P.R. China

21

22 Author Correspondence: [antony.rodriguez@bcm.edu](mailto:antony.rodriguez@bcm.edu)

23

24 **ABSTRACT**

25 Environmental air irritants including nanosized carbon black (nCB) can drive systemic  
26 inflammation, promoting chronic obstructive pulmonary disease (COPD) and emphysema  
27 development. The *let-7* family of miRNAs is associated with IL-17-driven T cell inflammation, a  
28 canonical signature of lung inflammation. Recent evidence suggests the *let-7* family is

29 downregulated in patients with COPD, however, how they cause emphysema remains unclear.  
30 Here we show that overall expression of the *let-7* miRNA clusters, *let-7b/let-7c2* and *let-7a1/let-*  
31 *7f1/let-7d*, are reduced in the lungs and T cells of smokers with emphysema as well as in mice  
32 with cigarette smoke (CS)- or nCB-elicited emphysema. We demonstrate that loss of the *let-7b/let-*  
33 *7c2*-cluster in T cells predisposed mice to exaggerated CS- or nCB-elicited emphysema.  
34 Furthermore, ablation of the *let-7b/let-7c2-cluster* enhanced CD8<sup>+</sup>IL17a<sup>+</sup> T cells (Tc17) formation  
35 in emphysema development in mice. Additionally, transgenic mice overexpressing *let-7* in T cells  
36 were resistant to Tc17 and CD4<sup>+</sup> T cells (Th17) development when exposed to nCB.  
37 Mechanistically, our findings reveal the master regulator of Tc17/Th17 differentiation, RAR-related  
38 orphan receptor gamma t (ROR $\gamma$ t), as a direct target of *let-7* miRNA in T cells. Overall, our findings  
39 shed light on the *let-7/ROR $\gamma$ t* axis as a braking and driving regulatory circuit in the generation of  
40 Tc17 cells and suggests a novel therapeutic approach for tempering the augmented IL-17-  
41 mediated response in emphysema.

42

## 43 INTRODUCTION

44 Chronic obstructive pulmonary disease (COPD) ranks as the third leading cause of  
45 mortality and is projected to account for over a billion deaths by the end of the twenty-first century  
46 (GBD Chronic Respiratory Disease Collaborators, 2020; *Findings from the Global Burden of*  
47 *Disease Study 2017, 2019*; Laniado-Laborín, 2009). Currently, there are no treatment options to  
48 reverse emphysema, the most clinically significant variant of COPD, which often is progressive  
49 despite smoking cessation (Bhavani et al., 2015; Anthonisen et al., 2002).

50 Inhalation of fine particulate matter smaller than 2.5 microns (PM<sub>2.5</sub>) found in outdoor and  
51 indoor air pollution as well as tobacco smoke are risk factors for COPD development (Adeloye et  
52 al., 2022; Eisner et al., 2010; Hu et al., 2010). We have previously shown that nano-sized carbon

53 black (nCB), a noxious chemical constituent of PM<sub>2.5</sub> found in the lungs of smokers, activates  
54 macrophages and dendritic cells orchestrating a pathogenic T cell-dependent inflammatory  
55 response and emphysema in mice (Lu et al., 2015; You et al., 2015; Shan et al., 2009; C.-Y.  
56 Chang et al., 2022).

57 Research over the last decade has pointed to the importance of dysfunctional  
58 inflammatory T cells in human COPD lung tissue and animal models of emphysema (Grumelli et  
59 al., 2004; Xu et al., 2012; Williams et al., 2021). Aberrant T cells are implicated in impaired host  
60 defense, exaggerated inflammation, and loss of self-tolerance in COPD (Williams et al., 2021;  
61 Chen et al., 2023; Hogg et al., 2004; Maeno et al., 2007; Xu et al., 2012). In this regard, we and  
62 others have demonstrated the role and pathogenicity of activated IFN- $\gamma$  and IL-17-secreting  
63 subsets of CD4<sup>+</sup> and CD8<sup>+</sup> T lymphocytes including Th1, Th17, and Tc1 cells in clinical isolates  
64 and in mice with COPD (Lu et al., 2015; You et al., 2015; Shan et al., 2009; S.-H. Lee et al., 2007;  
65 Kheradmand et al., 2023). The IL-17-secreting Th17 cells are particularly important as they  
66 promote the destruction of lung epithelium and recruitment of macrophages and neutrophils which  
67 then release proteolytic enzymes such as matrix metalloproteinases (MMPs) involved in the  
68 degradation of the lung structural matrix (Barnes, 2016; Hoenderdos & Condliffe, 2013). We  
69 previously demonstrated that intranasal inhalation of nCB in mice is sufficient to induce  
70 emphysema by stimulating T cell activation by dendritic cells and macrophages in mice. Moreover,  
71 we found that genetic ablation of IL-17a can attenuate nCB- or cigarette smoke-induced alveolar  
72 destruction and airway inflammation (Shan et al., 2012; You et al., 2015). More recently, IL-17A  
73 and IL-17F secreting CD8<sup>+</sup> T cell (Tc17) subpopulation has been shown to play a critical role in  
74 the pathogenesis of several autoimmune and inflammatory disorders (Globig et al., 2022; Huber  
75 et al., 2013; Srenathan et al., 2016).

76 Both Th17 and Tc17, require the fate-deterministic transcription factor RAR-related orphan  
77 receptor gamma t (ROR $\gamma$ t, encoded by *Rorc*) for differentiation and production of IL-17a (Ivanov

78 et al., 2007). ROR $\gamma$ t is the best-studied positive transcriptional regulator of IL-17a and IL-17f  
79 (Ivanov et al., 2006). In accordance with the importance of IL-17a transcription, ROR $\gamma$ t expression  
80 has also been reported to be elevated in COPD patients and in mouse models of COPD (Chu et  
81 al., 2011; Li et al., 2015). However, the upstream pathophysiologic mechanisms that contribute to  
82 the induction of ROR $\gamma$ t and differentiation of Tc17 cells in COPD have not been well elucidated.

83 We previously reported that *miR-22* inhibits HDAC4, promoting antigen-presenting cell  
84 activation (APC) in the lungs and inducing Th17-mediated emphysema in response to CS or nCB  
85 in mice (Lu et al., 2015). Additional miRNAs that control APC and/or T cell driven IL-17a<sup>+</sup>  
86 inflammation have been identified by others including the *let-7* miRNA family (Mai et al., 2012;  
87 Angelou et al., 2020). MicroRNA expression-based studies have shown frequent downregulation  
88 of members of the *let-7* miRNA family, including *let-7a*, *let-7b*, *let-7c*, *let-7d*, *let-7e*, and *let-7f* in  
89 human emphysematous lung tissue and in murine models of emphysema, but the mechanism(s)  
90 of action remain ill-defined (Christenson et al., 2013; Pottelberge et al., 2011; Conickx et al., 2017;  
91 Izzotti et al., 2009). *Let-7* microRNA genes are encoded across eight loci either as single genes  
92 or as polycistronic clusters which have confounded their analysis *in vivo* (Rodriguez et al., 2004).  
93 Previous studies used *Lin28b* transgenic overexpression in T cells to block the maturation and  
94 processing of the *let-7* miRNA family. They showed an inhibitory role of *let-7* family in Th17-driven  
95 response in murine model of experimental autoimmune encephalomyelitis (EAE) (Angelou et al.,  
96 2020).

97 Here we found that *let-7* miRNA, notably the *let-7a3/let-7b* and *let-7a1/let-7f1/let-7d*  
98 clusters, are suppressed in the T cells isolated from lungs of emphysema patients. Consistently,  
99 the analogous murine *let-7b/let-7c2- (let-7bc2)* and *let-7a1/f1/d1- (let-7afd)* clusters were similarly  
100 downregulated in pre-clinical emphysema models. We engineered mouse models with the  
101 specific loss-of-function (LOF) mutations of the *let-7bc2* or *let-7afd* clusters (*let-7bc2<sup>LOF</sup>* and *let-*  
102 *7afd<sup>LOF</sup>*, respectively) in T cells as well as an inducible *let-7g* gain-of-function (GOF) (*let-7<sup>GOF</sup>*)

103 model to determine the T cell-intrinsic role of *let-7* miRNA in emphysema pathogenesis. Deletion  
104 of *let-7* miRNA in T cells worsened alveolar damage elicited by inhalation of CS or nCB, and  
105 increased infiltration of immune cells in the airways, including IL-17-producing CD8<sup>+</sup> T (Tc17) cells.  
106 Mechanistically, we found that *let-7* controls type 17 differentiation by directly targeting the  
107 lineage-determining transcription factor, ROR $\gamma$ t. In support of this conclusion, *let-7*<sup>GOF</sup> mice were  
108 resistant to nCB-mediated induction of ROR $\gamma$ t and Tc17 responses. Thus, we show a previously  
109 unappreciated role for *let-7* miRNA as a repressor of ROR $\gamma$ t and a molecular brake to the IL-17a-  
110 mediated T cell inflammation in emphysema.

111

## 112 RESULTS

### 113 The *let-7bc2*- and *let-7afd*-clusters are downregulated in lungs and T cells in COPD.

114 To explore the involvement of *let-7* in emphysema, we scrutinized the genomic locations and  
115 transcriptional annotation of *let-7* members frequently downregulated in lung T cells isolated from  
116 smoker's lungs as well as mouse models of emphysema. This combined approach showed close  
117 linkage and high conservation of two *Let-7* clusters encoded from long intergenic non-coding RNA  
118 (linc)-like precursors in humans and mice (Figure 1A). To shed light on whether these *Let-7*  
119 clusters are downregulated in patients with COPD, we analyzed a published (GSE57148) lung  
120 RNA-seq dataset obtained from COPD (N=98 and control (N=91) subjects (Kim et al., 2015). Our  
121 analysis identified significant downregulation of the *Mirlet7ahg* and *Mirlet7bhg* gene cluster  
122 transcripts in COPD compared to control subjects (Figure 1B). We carried out quantitative PCR  
123 (qPCR) detection of *Let-7a*, which is encoded by both clusters, in lung tissue samples of smokers  
124 with emphysema and non-emphysema controls, detecting significant downregulation of *Let-7a* in  
125 emphysema samples relative to controls (Figure 1C). Because *Let-7* has been shown to  
126 participate in IL-17<sup>+</sup> T cell responses (Angelou et al., 2020; Guan et al., 2013; Newcomb et al.,

127 2015), we next sought to determine if the expression pattern of *Mirlet7ahg* and *Mirlet7bhg*-derived  
128 *Let-7* members are impaired in purified CD4<sup>+</sup> T cells from emphysematous lungs. In support of  
129 our original hypothesis, the CD4<sup>+</sup> T cell expression of *Let-7a*, *Let-7b*, *Let-7d*, and *Let-7f* were all  
130 inversely correlated with more severe emphysema distribution in the lungs as determined by CT  
131 scan (Figure 1D).

132 Next, we elucidated *let-7a1/let-7f1/let-7d*- and *let-7b/let-7c2*-clusters expression (herein  
133 referred to as *let-7afd* and *let-7bc2* respectively) in murine models of CS- or nCB-induced  
134 emphysema respectively (Figure 1E). Paralleling our observations in human COPD and  
135 emphysema, mice with CS- or nCB-induced emphysema exhibited reduced expression levels of  
136 *pri-let7afd* and *pri-let7bc2* transcripts in the lung and from isolated lung CD4<sup>+</sup> and CD8<sup>+</sup> T cells  
137 (Figure 1F,G,H). Collectively, our expression results indicate suppression of *let-7afd* and *let-7bc2*-  
138 clusters in the lung and T cells in human and pre-clinical models of emphysema.

139

#### 140 **Conditional deletion of the *let7bc2*-cluster in T cells enhances nCB- or CS-induced** 141 **emphysema.**

142 To investigate the *in vivo* requirement of the *let-7bc2*-cluster within T cells, we generated  
143 conditional ready floxed mice (*let-7bc2<sup>flox/flox</sup>*). We then crossed *let7-bc2<sup>flox/flox</sup>* mice with *CD4-Cre*  
144 mice to generate *let-7bc2<sup>flox/flox</sup>; CD4-Cre* LOF mice (denoted as *let-7bc2<sup>LOF</sup>* mice hereafter)  
145 (Figure 2A). This approach allowed us to conditionally delete the *let-7bc2* cluster in all T cells  
146 derived from the CD4<sup>+</sup>CD8<sup>+</sup> double-positive (DP) stage (P. Lee et al., 2001; Shi & Petrie, 2012).  
147 We confirmed that *let-7bc2<sup>LOF</sup>* mice exhibit robust conditional deletion of the *let-7bc2* cluster in  
148 DP thymocytes and peripheral CD8<sup>+</sup> T and CD4<sup>+</sup> T cells (Figure 2B and data not shown). Our *let-*  
149 *7bc2<sup>LOF</sup>* adult mice were born at the expected Mendelian frequency and did not show any overt  
150 histopathologic or inflammatory changes in lungs histopathology up to 1 year of age in comparison

151 to *let-7bc2<sup>ff</sup>* control mice (Figure 1-figure supplement 1A,B,C,D and data not shown).  
152 Furthermore, quantification of major immune populations and T cell subsets by flow cytometry in  
153 *let-7bc2<sup>LOF</sup>* were comparable to control mice under baseline conditions and with moderate aging  
154 (Figure 1-figure supplement 1A,B,C,D).

155 We next exposed *let-7bc2<sup>LOF</sup>* and *let-7bc2<sup>ff</sup>* control mice to nCB or CS and examined the  
156 lungs under the context of experimental emphysema. Histomorphometry measurements of mean  
157 linear intercept (MLI) from hematoxylin and eosin (H&E)-stained sections revealed that the  
158 enlargement of alveolar spaces sustained from either nCB- or CS-exposure was exaggerated in  
159 *let-7bc2<sup>LOF</sup>* mice relative to controls (Figure 2C-E). Chronic inflammation in emphysema is  
160 characterized by the recruitment of macrophages and neutrophils to the lung tissue and airways  
161 (Peleman et al., 1999; Senior & Anthonisen, 1998). Internally consistent with MLI measurements,  
162 *let-7bc2<sup>LOF</sup>* mice treated with nCB showed significantly increased airway infiltration of  
163 macrophages and neutrophils in BAL fluid as compared to wild-type control animals (Figure 2F).  
164 Concomitant with these findings, expression levels of *Mmp9* and *Mmp12*, which are secreted by  
165 macrophages and neutrophils to degrade elastin and mediate alveolar damage, were elevated in  
166 airways of *let-7bc2<sup>LOF</sup>* mice exposed to CS versus controls (Figure 2G). Collectively, our data  
167 suggests that the *let-7bc2*-cluster within T cells protects by dampening airway destruction and  
168 inflammation because the absence of this cluster worsens the severity of experimental  
169 emphysema in mice.

170

### 171 **The *let-7bc2* miRNA cluster negatively regulates T<sub>c</sub>17 inflammation in emphysema.**

172 We sought to identify the T cell-intrinsic mechanisms that underlie the exaggerated  
173 inflammation observed in emphysematous *let7bc2<sup>LOF</sup>* mice. We focused on the IL-17-mediated T  
174 cell response because it promotes neutrophil and macrophage recruitment in the lungs (Beringer

175 et al., 2016; Veldhoen, 2017; Shan et al., 2012). Previously, we established the induction of  
176 CD4<sup>+</sup>IL17<sup>+</sup> (Th17) cells along with CD4<sup>+</sup>IFN $\gamma$ <sup>+</sup> (Th1) cells in mice with chronic nCB exposure (You  
177 et al., 2015), however whether nCB similarly induces CD8<sup>+</sup>IL17a<sup>+</sup> T cells (Tc17) or cytotoxic T  
178 cells (Tc1) had not been studied. The flow cytometric profiling of lung T cells revealed enriched  
179 proportions and counts of Tc1 and Tc17 cells in mice with nCB-emphysema and we confirmed the  
180 induction of Th17 and Th1 cells (Figure 3A-B control PBS and control nCB). These findings  
181 suggests that nCB elicits both the type 17 and type 1 T cell responses, consistent with CS and  
182 elastase pre-clinical models of emphysema (Zhang et al., 2019).

183 We next interrogated the regulatory role of the *let-7bc2*-cluster in the type 17 and type 1  
184 responses generated from exposure to nCB. Interestingly, *let-7bc2*<sup>LOF</sup> mice showed increased  
185 CD8<sup>+</sup>IL17a<sup>+</sup> Tc17 cells relative to nCB control animals. In contrast, CD8<sup>+</sup>IFN<sup>+</sup> and GZMA<sup>+</sup> Tc1  
186 populations remained unperturbed with absence of the *let-7bc2* cluster, suggestive of a more  
187 refined regulatory role on Tc17 differentiation (Figure 3A-B). There were no significant differences  
188 in either Th1 or Th17 cells when comparing nCB-treated *let-7bc2*<sup>LOF</sup> to wild-type controls,  
189 indicating the *let-7bc2* cluster was dispensable for their generation (Figure 3C). Regulatory T cells  
190 form a dynamic axis with Tc17/Th17 cells and act as a counterbalance to lung inflammation in  
191 emphysema (Duan et al., 2016; Jin et al., 2014). Therefore, we examined whether Tc17 cell  
192 alterations were driven by the *let-7bc2* cluster acting on regulatory T cells (Tregs). The *let-7bc2*<sup>LOF</sup>  
193 mice showed no significant difference in Tregs subset relative to controls in our model (Figure  
194 3D). Together, our data support the notion that deletion of the *let-7bc2*-cluster is insufficient to  
195 provoke Tc17 cell generation under homeostatic conditions. However, under the context of chronic  
196 inflammation in emphysema, the loss of *let-7bc2*-cluster is intrinsic for the potentiation of T cells  
197 towards Tc17 differentiation.

198 **The *let-7* family directly inhibits ROR $\gamma$ t expression governing Tc17 differentiation in**  
199 **emphysema.**



200 We utilized the TargetScan predictive algorithm to identify putative *let-7* microRNA targets  
201 that are known to control the IL-17-mediated T cell response (Agarwal et al., 2015). This analysis  
202 revealed that the 3'UTR region of *Rorc*, encoding ROR $\gamma$ t, contains an evolutionarily conserved  
203 and complementary motif for the *let-7* miRNA family (Figure 4A). Thus, we examined if *let7bc2*-  
204 cluster loss in T cells would stimulate and enhance ROR $\gamma$ t. Initially, we carried out flow cytometric  
205 quantification for ROR $\gamma$ t in thymocyte, splenic, and lung T cells of naïve control and *let7bc2<sup>LOF</sup>*  
206 mice up to 6-months of age. Our interrogation of ROR $\gamma$ t mean fluorescent intensity (MFI) by flow  
207 cytometry showed induction of ROR $\gamma$ t in single-positive CD8<sup>+</sup> and CD4<sup>+</sup> thymocytes, as well as  
208 peripheral splenic CD8<sup>+</sup> and CD4<sup>+</sup> T cells (Figure 4B). However, ROR $\gamma$ t levels appeared  
209 unchanged in purified lung CD8<sup>+</sup> T cells and CD4<sup>+</sup> T cells of naive *let-7bc2<sup>LOF</sup>* mice, alluding to a  
210 compensatory effect in homeostatic lung T cells (Figure 4B). Since we and others have shown  
211 that miRNAs are frequently associated with stress-dependent phenotypes, we posited that  
212 emphysematous *let-7bc2<sup>LOF</sup>* T cells are poised towards induction of ROR $\gamma$ t and production of  
213 IL17<sup>+</sup> subsets after challenge with nCB. Indeed, nCB-emphysematous *let-7bc<sup>LOF</sup>* mice exhibited  
214 enhanced ROR $\gamma$ t protein levels in both CD8<sup>+</sup> and CD4<sup>+</sup> T cells relative to control mice with  
215 emphysema (Figure 4C).

216 Because we had found that the *let-7afd*-cluster is downregulated in T cells isolated from  
217 COPD lungs in human and mice, and that the *let-7* family operates with some functional  
218 redundancy, we generated mice with conditional deletion of the *let7afd*-cluster in T cells (*let-7afd<sup>ff</sup>*;  
219 *CD4-Cre*). The *let-7afd<sup>ff</sup>*; *CD4-Cre* (*let7afd<sup>LOF</sup>*) mice aged up to 6-months did not exhibit lung  
220 histopathology nor inflammatory changes (data not shown). Of particular interest, ablation of the  
221 *let-7afd*-cluster enhanced levels of ROR $\gamma$ t in thymic and peripheral T cells of mice (Figure 4D).  
222 Overall, this indicates that independent *let-7* clusters restrain ROR $\gamma$ t expression levels from  
223 thymic development to peripheral T cells under homeostatic conditions. Next, we determined  
224 whether loss of *let-7afd*-cluster in T cells likewise sensitizes mice towards induction of ROR $\gamma$ t in

225 nCB-emphysema. Intranasal administration of nCB provoked increased ROR $\gamma$ t expression in lung  
226 T cells of *let-7afd*<sup>LOF</sup> mice as compared to *let-7afd*<sup>ff</sup> control mice (Figure 4E), supporting  
227 overlapping functionality between the *let-7bc2* and *let-7afd*-clusters in repression of ROR $\gamma$ t within  
228 T cells.

229 To confirm that the *let-7* family negatively regulates Tc17 cell differentiation, at least in part,  
230 cell autonomously in CD8<sup>+</sup> T cells, we purified naïve CD8<sup>+</sup> T cells from *let-7bc2*<sup>LOF</sup> and control  
231 mice spleens and cultured these cells *in vitro* in the presence of Tc17 polarizing (TGF $\beta$ , IL-6, anti-  
232 IFN $\gamma$ , IL-23, and IL-1 $\beta$ ) or Tc1 polarizing (IL-2) conditions (Flores-Santibáñez et al., 2018). Our  
233 flow cytometric analysis confirmed the enhanced commitment of *let-7*-cluster deficient CD8<sup>+</sup> T  
234 cells towards Tc17 cells and IL-17a<sup>+</sup> production relative to control CD8<sup>+</sup> T cells (Figure 5A-B).  
235 Moreover, enhanced Tc17 cell differentiation mirrored the increased IL-17a detected in the  
236 supernatant from *in vitro* polarized cells as quantified by ELISA (Figure 5C). Parallel assessment  
237 of Tc1 differentiation did not detect a difference in CD8<sup>+</sup>IFN $\gamma$ <sup>+</sup> cells (Figure 5A and Figure 5D).  
238 Altogether, these data recapitulated our *in vivo* findings that the *let-7bc2* cluster negatively  
239 regulates Tc17 response but is dispensable in Tc1 cells. Finally, to determine whether Tc17  
240 differentiation is likewise controlled by the *let-7afd* cluster, we cultured naïve CD8<sup>+</sup> splenocytes  
241 from *let-7afd*<sup>LOF</sup> and controls under Tc17 conditions. As we had observed with *let-7bc2*<sup>LOF</sup>,  
242 absence of the *let-7afd* cluster in T cells further enhanced differentiation towards Tc17 cells as  
243 quantified by flow cytometry and ELISA (Figure 5E-F).

244 Next, we focused on *Rorc* as a potential direct target of *let-7*, which could mechanistically  
245 mediate enhanced Tc17 differentiation in *let7bc2*<sup>LOF</sup> mice. Towards this objective, tested whether  
246 *let-7bc2*<sup>LOF</sup> naïve CD8<sup>+</sup> T cells show elevated ROR $\gamma$ t expression under either Tc0 or Tc17  
247 differentiation conditions. In agreement with enhanced Tc17 differentiation, ROR $\gamma$ t expression  
248 was differentially and significantly upregulated under both Tc0 and Tc17 differentiation conditions  
249 in *let-7bc2*<sup>LOF</sup> cells relative to controls (Figure 5G). To determine whether *let-7* directly represses

250 *Rorc* mRNA levels we cloned the 3'UTR of *Rorc* into luciferase constructs. These reporter assays  
251 with *let-7b* expressing cells independently confirmed that *let-7b* represses *Rorc* (Figure 5H, left).  
252 Furthermore, deletion of the putative *let-7* binding sequence (Figure 4A) abrogated repression  
253 by *let-7b* (Figure 5H, right), thus confirming *Rorc* as a functional target of *let-7* miRNA. Overall,  
254 these *in vitro* experiments readily recapitulated an upstream regulatory role for *let-7* in Tc17  
255 differentiation, mediated in part, via direct suppression of ROR $\gamma$ t.

256

### 257 **Enforced expression of *let-7* tempers ROR $\gamma$ t T cell expression levels in experimental** 258 **emphysema.**

259 To explore a potential protective role of *let-7* miRNA in experimentally induced  
260 emphysema, we generated mice which allowed for selective induction of *let-7* activity in T cells  
261 using the published *rtTA-iLet7* mice (Zhu et al., 2011; Belteki et al., 2005). We bred the *rtTA-iLet7*  
262 mice to *CD4-Cre* (here in referred to as *let-7<sup>GOF</sup>*) to allow Cre-loxP/doxycycline dependent *let-7g*  
263 overexpression in thymic DP-derived T cells (Figure 6A). Steady-state *let-7<sup>GOF</sup>* and control (*rtTA-*  
264 *iLet7*) mice were examined for compromised ROR $\gamma$ t protein levels within thymocytes and  
265 peripheral T cells. Providing further evidence of *let-7*-dependent regulation of *Rorc*, protein levels  
266 of ROR $\gamma$ t were suppressed in CD8<sup>+</sup> and CD4<sup>+</sup> T cells of *let-7<sup>GOF</sup>* mice relative to controls (Figure  
267 6B). To determine whether enforced expression of *let-7* offered protection from experimental  
268 emphysema, *let-7<sup>GOF</sup>* and control mice were treated with nCB and then examined for changes in  
269 lung pathology and T cell type 17 responses. The *let-7<sup>GOF</sup>* mice did not exhibit any signs of lung  
270 inflammation or pathologic remodeling at baseline (Figure 6C-D and data not shown)  
271 Histopathologic analysis revealed a comparable degree of lung alveolar distension via  
272 morphometric measurements of MLI in nCB-treated *let-7<sup>GOF</sup>* mice versus controls suggesting that  
273 enforced *let-7* expression is insufficient to protect the lung from emphysema (Figure 6C-D). On  
274 the other hand, evaluation of IL17<sup>+</sup> response and ROR $\gamma$ t levels in emphysematous lung T cells

275 demonstrated that, in contrast to control nCB-treated mice, *let-7<sup>GOF</sup>* mice exhibited dampened  
276 lung Tc17 and Th17 cell populations and were resistant to the induction of ROR $\gamma$ t after nCB-  
277 exposure (Figure 6F-6E). Taken together, our *let-7* LOF and GOF models demonstrate the  
278 necessity and sufficiency of *let-7* miRNA to act as a molecular brake to the type 17 T cell response  
279 through the direct regulation of ROR $\gamma$ t, further our data suggests that nCB- or CS-mediated  
280 suppression of this braking mechanism furthers inflammation and exacerbates emphysema  
281 severity (Figure 6G).

282

## 283 **DISCUSSION**

284 MiRNA expression-based studies of COPD patients and mice exposed to CS have  
285 reported downregulation of *let-7* miRNA expression in lung tissues (Conickx et al., 2017;  
286 Christenson et al., 2013b; Schembri et al., 2009). We and others explored the consequence of  
287 loss of *let-7* expression/activity with synthetic oligonucleotides, sponges, lentiviral antisense  
288 knockdown, or via ectopic delivery of Lin28b (Polikepahad et al., 2010; Viswanathan et al., 2008;  
289 Piskounova et al., 2011), but studies pinpointing the role of individual *let-7* clusters as potential  
290 drivers of lung inflammation and COPD within T cells remained elusive. In the present study, we  
291 established that the *let-7* miRNA family members encoded by the *let-7bc2*- and *let-7afd*-clusters  
292 are downregulated in T cells from lungs of emphysema patients and emphysematous mice that  
293 were exposed to CS or nCB. Correspondingly, we demonstrated that *in vivo* genetic ablation of  
294 *let-7bc2-cluster* further sensitized mice to lung tissue destruction and emphysema upon treatment  
295 with nCB or CS. Mechanistically, our studies suggests that *let-7* miRNA prevents the emergence  
296 of CD8<sup>+</sup> T cell differentiation into Tc17 cells during emphysema in part, by directly silencing of  
297 *Rorc*.

298 Tc17 cells are vital for defense against viral, fungal, and bacterial infections and they have  
299 also been associated with inflammation in various human diseases such as multiple sclerosis,  
300 inflammatory bowel disease, and cancer (Huber et al., 2013; Globig et al., 2022; Corgnac et al.,  
301 2020). In accordance with the potential pathogenic role of Tc17 cells as drivers of COPD, several  
302 studies detected increased cell numbers in airways and tissues of COPD patients as well as lungs  
303 of smoke-exposed animal models (Chang et al., 2011; Zhou et al., 2020; Duan et al., 2013). Other  
304 researchers also detected increased Tc17 subpopulations in tissues of COPD patients with  
305 infectious microbial exacerbations. In our earlier work to define the adaptive T cell immune  
306 responses in nCB induced COPD, we predominantly focused on the pathogenic role of Th17 cells,  
307 but did not examine Tc17 cells (You et al., 2015). Here we expand upon our prior observations,  
308 revealing that chronic exposure to nCB and elicitation of emphysema mice orchestrates the  
309 emergence and accumulation of Tc17 cells which may act in parallel with Th17 cells to promote  
310 tissue damage.

311 Although ROR $\gamma$ t has been the subject of intense scrutiny and is subject to extensive  
312 transcriptional and post-transcriptional regulatory control, to our knowledge this is the first  
313 reported demonstration of miRNA-mediated gene silencing to ROR $\gamma$ t. Our data also showed that  
314 *in vivo* conditional genetic ablation of individual *let-7* clusters in T cells stimulates a rise in ROR $\gamma$ t  
315 protein expression in single-positive thymocytes and peripheral CD8<sup>+</sup> and CD4<sup>+</sup> T cells while  
316 enforced *let-7* activity leads to partial repression of ROR $\gamma$ t in T cells. Despite these alterations in  
317 ROR $\gamma$ t expression in our *let-7* T cell LOF and GOF mice, the mice did not exhibit spontaneous  
318 gross phenotypes in thymus, spleens, or lungs at baseline. This may be due to the subtle and  
319 modest expression thresholding of ROR $\gamma$ t detected in mice and/or residual *let-7* expression in T  
320 cells. On the other hand, and in agreement with our Tc17 and experimental emphysema data, we  
321 observed enhanced ROR $\gamma$ t expression and IL-17a<sup>+</sup>CD8<sup>+</sup> T cells in lungs of *let-7* LOF mice after  
322 treatment with nCB. We corroborated the importance of *let-7* activity in Tc17 differentiation of ex

323 *in vivo* cultured CD8<sup>+</sup> T cells, as well as in the direct posttranscriptional control of ROR $\gamma$ t, suggesting  
324 that this defect, is in part, direct and cell autonomous. Interestingly, even though ROR $\gamma$ t was  
325 elevated in lung CD4<sup>+</sup> T cells to a similar extent as CD8<sup>+</sup> T cells, the enhanced IL17<sup>+</sup> responses  
326 were limited to Tc17 subpopulation in the *let-7bc2*<sup>LOF</sup> mice. Although, the *let-7afd*<sup>LOF</sup> mice also  
327 showed baseline induction of ROR $\gamma$ t relative to controls in lung T cells the mice did not exhibit  
328 changes in Tc17/Th17 subpopulations (data not shown). Nonetheless, it seems likely that under  
329 different cellular contexts, the functions of *let-7*-clusters do not fully overlap in association with  
330 differential thresholding of mRNA targets. Indeed, in B cells, the *let-7afd*-cluster is essential for an  
331 antigen-specific antibody response, whereas the *let-7bc2*-cluster appears dispensable (Jiang et  
332 al., 2018), iterating that differential physiological role of *let-7* clusters in the immune system and  
333 validating an individual cluster approach in dissemination of mechanisms of *let-7* in T cells. ROR $\gamma$ t  
334 is a defining transcription factor of the IL-17-secreting subset of immune cells, which also includes  
335  $\gamma\delta$ 17 T cells, NKT17 and type 3 innate lymphoid cells, populations that contribute to COPD  
336 pathology (Yanagisawa et al., 2017). A limitation of our study is that we did not examine whether  
337 these populations were impacted by nCB-emphysema and/or in the context of *let-7* LOF.

338 Published studies revealed a protective role of *let-7* family against Th17-driven pathogenic  
339 response in EAE attributed in part to direct regulation of *IL-1 receptor 1* and *IL-23 receptor*  
340 (Angelou et al., 2020). Lending some support to these observations, we detected subtle transcript  
341 level induction of *Il23r* in *let-7bc2*<sup>LOF</sup> *in vitro* polarized Tc17 cells (data not shown). However, prior  
342 publications on the role of *let-7* in T cells made use of *in vivo* *Lin28b* transgenic overexpression  
343 in immune cells to block maturation and activity of the entire *let-7* miRNA family. Furthermore,  
344 *Lin28b* was recently reported to influence transcriptome-wide ribosome occupancy and global  
345 miRNA biogenesis (Tan et al., 2019) which could account for differences in scope of *let-7* targets  
346 in those studies and ours. Nonetheless, further studies will be required to ascertain whether other

347 targets of *let-7* beyond ROR $\gamma$ t synergistically potentiate the *in vivo* Tc17-response and  
348 emphysema phenotype in *let7-bc2<sup>LOF</sup>* T cells.

349 Tc17 cells play a major role in microbial infections, providing a potent anti-viral response  
350 (Hamada et al., 2009; Yeh et al., 2010), while viral infection has been an established factor in  
351 COPD exacerbations (Hewitt et al., 2016; Wedzicha, 2004). It will be interesting to determine  
352 whether loss of *let-7bc2* or *let-7afd*-cluster activity in the T cell compartment contributes to COPD  
353 disease susceptibility in the context of viral exposure. Our experiments with *let-7* GOF were  
354 partially successful in limiting the emergence of Tc17 and Th17 in nCB-elicited emphysema but it  
355 did not protect the lung from alveolar remodeling. Additional, studies will be required to ascertain  
356 whether interventions that enhance *let-7* activity are successful in acute models of CS exposure  
357 and COPD or in other chronic inflammation diseases associated with dysregulation of ROR $\gamma$ t and  
358 IL17<sup>+</sup> injury.

359

## 360 **MATERIALS AND METHODS**

### 361 **Mice**

362 Conditional knockout-ready floxed *let-7bc2* and *let-7afd* mice were generated using CRISPR gene  
363 editing in an isogenic C57BL/6 genetic background and were sequence verified for rigor. Mice  
364 were PCR genotyped from ear samples with primers flanking loxP sites (Supplementary Table).  
365 The *let-7bc2<sup>fllox/fllox</sup>*, *CD4-cre* and *let-7afd<sup>fllox/fllox</sup>*, *CD4-cre* mice were PCR genotyped. The *R26-*  
366 *STOP-rtTA*; *Col1a1-tet0-let-7 (rtTA-iLet7)* mice were obtained from JAX Jax Stocks 023912 and  
367 05670 and then bred to *CD4-Cre* were PCR genotyped with established JAX primers. Control  
368 *rtTA-iLet7* and the *let-7<sup>GOF</sup>* mice were fed *ad libitum* with 200mg/kg of doxycycline-containing chow  
369 (Bio-Serv S3888) at weaning age. Syngeneic littermates served as controls for all mouse  
370 experiments. All mice were bred in the transgenic animal facility at Baylor College of Medicine. All  
371 experimental protocols used in this study were approved by the Institutional Animal Care and Use

372 Committee of Baylor College of Medicine animal protocol (AN-7389) and followed the National  
373 Research Council Guide for the Care and Use of Laboratory Animals.

374

### 375 **Human emphysema tissue samples and T cell isolation**

376 Lung tissues were obtained from a total of 28 non-atopic current or former smokers with significant  
377 (>20 pack-years, one pack-year equals to smoking one pack of cigarettes per day each year)  
378 history of smoking who were recruited into studies from the chest or surgical clinics at Michael E.  
379 DeBakey Houston Veterans Affairs Medical Center hospitals (Shan et al., 2009). Human lung  
380 single T cells were prepared from surgical resection and lungs in patients as previously described  
381 by selection with biotin-labeled antibodies by autoMACs (Miltenyi Biotec) (Yuan et al., 2020;  
382 Grumelli et al., 2004). Studies were approved by the Institutional Review Board at Baylor College  
383 of Medicine and informed consent was obtained from all patients. Emphysema and non-  
384 emphysema control patients were diagnosed from CT scans according to the criteria  
385 recommended by the National Institutes of Health–World Health Organization workshop summary  
386 (Pauwels et al., 2001).

387

### 388 **Human lung transcriptome data**

389 A publicly available RNA-seq dataset from a Korean cohort GSE57148 was selected for the  
390 analysis (Kim et al., 2015). The raw FASTQ files of paired end reads representing the  
391 transcriptome of control and cases were retrieved from the GEO database at the National Centre  
392 for Biological Information (NCBI) through accession number GSE57148 and analyzed with R  
393 package for differential expression.

394

### 395 **Cigarette smoke exposure model of pulmonary emphysema**

396 To promote emphysema, mice were exposed to cigarette smoke using our custom designed  
397 whole-body inhalation system (Morales-Mantilla et al., 2020). In total, mice were exposed to four



398 cigarettes (Marlboro 100's; Philip Morris USA) per day, five days a week, for four months as  
399 previously described (Morales-Mantilla et al., 2020, Shan et al., 2012).

400

#### 401 **nCB exposure model of pulmonary emphysema**

402 Nano-sized particulate carbon black was prepared and administered as previously described (You  
403 et al., 2015; Lu et al., 2015). Dried nCB nanoparticles were resuspended in sterile PBS to a  
404 concentration of 10 mg/ml. Fifty  $\mu$ l of reconstituted nCB (0.5 mg) were intranasally delivered to  
405 deeply anesthetized mice on a schedule of three times a week for four weeks (total delivered  
406 dose of 6 mg). Lung histomorphometry and airway inflammation were assessed four weeks after  
407 the final nCB challenge. For histomorphometric analysis, mice lungs were fixed with 10% neutral-  
408 buffered formalin solution via a tracheal cannula at 25-cm H<sub>2</sub>O pressure followed by paraffin  
409 embedding and tissue sectioning and stained with hematoxylin and eosin. Mean linear intercept  
410 (MLI) measurement of mouse lung morphometry were done as previously described (Shan et al.,  
411 2014; Morales-Mantilla et al., 2020). Briefly, this was done in a blinded fashion to mice genotypes  
412 from ten randomly selected fields of lung parenchyma sections. Paralleled lines were placed on  
413 serial lung sections and MLI was calculated by multiplying the length and the number of lines per  
414 field, divided by the number of intercepts (Morales-Mantilla et al., 2020).

415 BALF was collected by instilling and withdrawing 0.8 ml of sterile PBS twice through the  
416 trachea. Total and differential cell counts in the BALF were determined with the standard  
417 hemocytometer and HEMA3 staining (Biochemical Sciences Inc, Swedesboro, NJ) using 200  $\mu$ L  
418 of BALF for cytopspin slide preparation (Morales-Mantilla et al., 2020; Lu et al., 2015).

419

#### 420 **Cell isolation from murine lung tissue**

421 Mouse lung tissue were cut into 2-mm pieces and digested with collagenase type D (2 mg/ml;  
422 Worthington) and deoxyribonuclease (DNase) I (0.04 mg/ml; Roche) for 1 hour in a 37°C  
423 incubator. Single-cell suspensions from lung digest, spleen, and thymus were prepared by

424 mincing through 40- $\mu$ m cell strainers then washing and resuspension in complete RPMI media.  
425 Mouse lung and spleen single-cell suspensions were additionally overlaid on Lympholyte M cell  
426 separation media (Cedarlane) as indicated in the manufacturer's protocol to purify lymphocytes.  
427 For murine *let-7* expression studies, lung single-cell suspensions were labeled with anti-CD4<sup>+</sup> or  
428 anti-CD8<sup>+</sup> magnetic beads and separated by autoMACS (Miltenyi Biotec), or CD4<sup>+</sup>CD8<sup>+</sup> double  
429 positive cells purified from thymus single-cell suspensions by flow-cytometric sorting on FACS  
430 Aria (BD Biosciences).

431

### 432 ***In vitro* polarization of CD8<sup>+</sup> T cells**

433 CD8<sup>+</sup> naïve T cells were isolated from spleen using Mojosort Mouse CD8 Naïve T cell isolation  
434 Kit (Biolegend) and adjusted to a concentration of  $1.0 \times 10^6$  cells/mL. Purified cells were activated  
435 with plate-bound anti-CD3 (1.5 $\mu$ g/mL) and complete RPMI media containing anti-CD28  
436 (1.5 $\mu$ g/mL) and  $\beta$ -mercaptoethanol (50nM) for Tc0 polarization, or further supplemented with Tc1  
437 [IL-2 (10ng/mL)] or Tc17 [TGF $\beta$  (2ng/mL), IL-6 (20ng/mL), anti-IFN $\gamma$  (10 $\mu$ g/mL), IL-23 (20ng/mL),  
438 and IL-1 $\beta$  (5ng/mL)] polarization conditions for 72 hours (Flores-Santibáñez et al., 2018).

439

### 440 **ELISA**

441 Supernatant was collected from *in vitro* polarized murine CD8<sup>+</sup> T cells and centrifuged to remove  
442 cellular debris. Cytokine levels of IL-17a and IFN $\gamma$  were quantified from collected supernatant  
443 using Mouse IL-17a Uncoated ELISA and Mouse IFN gamma Uncoated ELISA (Invitrogen) Kits,  
444 respectively, per the manufacturer's instructions with colorimetric analysis by the Varioskan LUX  
445 microplate reader (ThermoFisher).

446

### 447 **Flow cytometric analysis**

448 Cells used for *in vitro* or *in vivo* cytokine analysis were stimulated with PMA (20ng/mL; Sigma  
449 Aldrich), Ionomycin (1 $\mu$ g/mL; Sigma Aldrich), and Brefeldin A (2 $\mu$ g/mL; Sigma Aldrich) for 4 hours

450 prior to flow staining (Lu et al., 2015). For intracellular staining, cells were fixed and permeabilized  
451 using the Mouse FOXP3 Buffer Set (BD) per the manufacturer's protocol. The fluorophore-  
452 conjugated antibodies used in this study were as follows: Live/Dead Fix Blue (Invitrogen), CD3  
453 PerCPCy5.5 (Biolegend), TCRb PE/Cy7 (Biolegend), CD4 PB (Biolegend), CD4 AF700  
454 (Biolegend), CD8 BV650 (Biolegend), CD25 BV421 (Biolegend), FOXP3 AF488 (Biolegend),  
455 ROR gamma T PE (Invitrogen), TCF1 AF647 (Cell Signaling Technologies), TCF1 PE (Biolegend),  
456 IFN $\gamma$  AF647 (Biolegend), IL17a FITC (Biolegend), IL17a PE (ebioscience), PD1 BUV737 (BD),  
457 TIM3 AF647 (R&D). Samples were analyzed using BD LSR II flow cytometer (BD Biosciences)  
458 and FlowJo software (TreeStar),

459

#### 460 **RNA Isolation and Quantitative RT-PCR**

461 RNA was isolated using miRNeasy (Qiagen) or RNeasy Mini Kit (Qiagen) in conjunction with the  
462 RNase-Free DNase (Qiagen) according to the manufacturer's instructions. cDNA of miRNAs and  
463 mRNAs were synthesized using TaqMan Advanced miRNA cDNA Synthesis Kit (ThermoFisher)  
464 and High-Capacity cDNA Reverse Transcription Kit Real-Time PCR system (Applied Biosystems).  
465 18S and snoRNA-202 were used to normalize mRNA and miRNA expression respectively.  
466 Quantitative RT-PCR data were acquired on 7500 Real-Time PCR System or StepOne Real-Time  
467 PCR System (Applied Biosystems) with the following TaqMan probes: *hsa-let-7a* [000377], *hsa-*  
468 *let-7b* [000378], *hsa-let-7d* [002283], *hsa-let-7f* [000382], *pri-miR-let7a* [Mm03306744\_pri], *pri-*  
469 *miR-let7d* [Mm03306666\_pri], *pri-miR-let7b* [Mm03306756\_pri], *Mmp9* [Mm00442991], *Mmp12*  
470 [Mm00500554].

471

#### 472 **Luciferase reporter assays**

473 Genomic fragment containing the murine *Rorc* 3'UTR was cloned into psiCHECK2 luciferase  
474 reporter plasmid (Promega). This construct was also used to generate the *let-7* 'seed' deletion  
475 mutant derivative using the QuikChange Multi Site Mutagenesis Kit (catalog 200514-5,

476 Stratagene). 3T3 mouse embryonic fibroblasts (MEFs) were transfected using Oligofectamine  
477 (Invitrogen) with 100 ng of psiCheck-2 plasmid containing wild-type or mutant 3'UTR, along with  
478 the miRNA control or *let-7b* duplex (Dharmacon) at a final concentration of 6 nM (Gurha et al.,  
479 2012). Reporter activity was detected with the Dual-Luciferase Reporter Assay System  
480 (Promega).

481

## 482 **Statistical analysis**

483 Statistical analyses were performed using GraphPad Prism 10.0.1 software. Statistical  
484 comparison between groups was performed using the unpaired Student's t-test, two-way analysis  
485 of variance (ANOVA) with Tukey's or Sidak's correction, and Mann-Whitney Test when indicated.  
486 A P-value less than 0.05 was considered statistically significant; ns indicates not significant.  
487 Statistical significance values were set as \* $p < 0.05$ , \*\* $p < 0.01$ , \*\*\* $p < 0.001$ , and \*\*\*\* $p < 0.0001$ .  
488 Data are presented as means  $\pm$  SEM. P-value and sample sizes (n) are indicated in the figure  
489 legends.

490

## 491 **COMPETING INTEREST STATEMENT**

492 The authors declare no competing interests.

493

## 494 **ACKNOWLEDGEMENTS**

495 We thank Jason Heaney and Denise Lanza at BCM Genetically Engineered Rodents Core  
496 (funded in part by NIH P30 CA125123); Patricia Castro at Tissue Acquisition and Pathology Core  
497 (funded in part by P30 CA125123); and Joel M. Sederstrom at the BCM and Cell Sorting Core  
498 with funding from the CPRIT Core Facility Support Award (CPRIT-RP180672) and NIH  
499 (CA125123 and RR024574). This work was supported by grants from the NHLBI (R01HL140398  
500 to AR), the Gilson Longenbaugh Foundation (to A.R.), and NIEHS (T32 ES027801 to PE).

501

502 **AUTHOR CONTRIBUTIONS**

503 P.E., X.H., D.B.C, F.K., and A.R. conceptualized experiments and interpreted results. P.E., X.H.,  
504 M.J.S., H.T., M.A.P., and S.L.L. acquired the data, M.J.R. provided bioinformatics analyses. P.E.  
505 and A.R. wrote the manuscript.

506

507 **REFERENCES**

508 Agarwal, V., Bell, G. W., Nam, J.-W., & Bartel, D. P. (2015). Predicting effective microRNA  
509 target sites in mammalian mRNAs. *eLife*, 4, e05005. <https://doi.org/10.7554/eLife.05005>

510 Angelou, C. C., Wells, A. C., Vijayaraghavan, J., Dougan, C. E., Lawlor, R., Iverson, E.,  
511 Lazarevic, V., Kimura, M. Y., Peyton, S. R., Minter, L. M., Osborne, B. A.,  
512 Pobezinskaya, E. L., & Pobezinsky, L. A. (2020). Differentiation of Pathogenic Th17  
513 Cells Is Negatively Regulated by Let-7 MicroRNAs in a Mouse Model of Multiple  
514 Sclerosis. *Frontiers in Immunology*, 10, 3125. <https://doi.org/10.3389/fimmu.2019.03125>

515 Barnes, P. J. (2016). Inflammatory mechanisms in patients with chronic obstructive pulmonary  
516 disease. *Journal of Allergy and Clinical Immunology*, 138(1), 16–27.  
517 <https://doi.org/10.1016/j.jaci.2016.05.011>

518 Beringer, A., Noack, M., & Miossec, P. (2016). IL-17 in Chronic Inflammation: From Discovery  
519 to Targeting. *Trends in Molecular Medicine*, 22(3), 230–241.  
520 <https://doi.org/10.1016/j.molmed.2016.01.001>

521 Chang, Y., Nadigel, J., Boulais, N., Bourbeau, J., Maltais, F., Eidelman, D. H., & Hamid, Q.  
522 (2011). CD8 positive T cells express IL-17 in patients with chronic obstructive  
523 pulmonary disease. *Respiratory Research*, 12(1), 43. [https://doi.org/10.1186/1465-9921-](https://doi.org/10.1186/1465-9921-12-43)  
524 12-43

- 525 Christenson, S. A., Brandsma, C.-A., Campbell, J. D., Knight, D. A., Pechkovsky, D. V., Hogg,  
526 J. C., Timens, W., Postma, D. S., Lenburg, M., & Spira, A. (2013a). miR-638 regulates  
527 gene expression networks associated with emphysematous lung destruction. *Genome*  
528 *Medicine*, 5(12), 114. <https://doi.org/10.1186/gm519>
- 529 Christenson, S. A., Brandsma, C.-A., Campbell, J. D., Knight, D. A., Pechkovsky, D. V., Hogg,  
530 J. C., Timens, W., Postma, D. S., Lenburg, M., & Spira, A. (2013b). miR-638 regulates  
531 gene expression networks associated with emphysematous lung destruction. *Genome*  
532 *Medicine*, 5(12), 114. <https://doi.org/10.1186/gm519>
- 533 Chu, S., Zhong, X., Zhang, J., Lao, Q., He, Z., & Bai, J. (2011). The expression of Foxp3 and  
534 ROR gamma t in lung tissues from normal smokers and chronic obstructive pulmonary  
535 disease patients. *International Immunopharmacology*, 11(11), 1780–1788.  
536 <https://doi.org/10.1016/j.intimp.2011.06.010>
- 537 Conickx, G., Avila Cobos, F., van den Berge, M., Faiz, A., Timens, W., Hiemstra, P. S., Joos, G.  
538 F., Brusselle, G. G., Mestdagh, P., & Bracke, K. R. (2017). microRNA profiling in lung  
539 tissue and bronchoalveolar lavage of cigarette smoke-exposed mice and in COPD  
540 patients: A translational approach. *Scientific Reports*, 7(1), Article 1.  
541 <https://doi.org/10.1038/s41598-017-13265-8>
- 542 Corgnac, S., Malenica, I., Mezquita, L., Auclin, E., Voilin, E., Kacher, J., Halse, H., Grynszpan,  
543 L., Signolle, N., Dayris, T., Leclerc, M., Droin, N., de Montpréville, V., Mercier, O.,  
544 Validire, P., Scoazec, J.-Y., Massard, C., Chouaib, S., Planchard, D., ... Mami-Chouaib,  
545 F. (2020). CD103+CD8+ TRM Cells Accumulate in Tumors of Anti-PD-1-Responder  
546 Lung Cancer Patients and Are Tumor-Reactive Lymphocytes Enriched with Tc17. *Cell*  
547 *Reports Medicine*, 1(7), 100127. <https://doi.org/10.1016/j.xcrm.2020.100127>

548 Duan, M.-C., Tang, H.-J., Zhong, X.-N., & Huang, Y. (2013). Persistence of Th17/Tc17 Cell  
549 Expression upon Smoking Cessation in Mice with Cigarette Smoke-Induced Emphysema.  
550 *Journal of Immunology Research*, 2013, e350727. <https://doi.org/10.1155/2013/350727>

551 Duan, M.-C., Zhang, J.-Q., Liang, Y., Liu, G.-N., Xiao, J., Tang, H.-J., & Liang, Y. (2016).  
552 Infiltration of IL-17-Producing T Cells and Treg Cells in a Mouse Model of Smoke-  
553 Induced Emphysema. *Inflammation*, 39(4), 1334–1344. [https://doi.org/10.1007/s10753-](https://doi.org/10.1007/s10753-016-0365-8)  
554 [016-0365-8](https://doi.org/10.1007/s10753-016-0365-8)

555 *Findings from the Global Burden of Disease Study 2017*. (2019, January 4). Institute for Health  
556 Metrics and Evaluation. [https://www.healthdata.org/policy-report/findings-global-](https://www.healthdata.org/policy-report/findings-global-burden-disease-study-2017)  
557 [burden-disease-study-2017](https://www.healthdata.org/policy-report/findings-global-burden-disease-study-2017)

558 Globig, A.-M., Hipp, A. V., Otto-Mora, P., Heeg, M., Mayer, L. S., Ehl, S., Schwacha, H.,  
559 Bewtra, M., Tomov, V., Thimme, R., Hasselblatt, P., & Bengsch, B. (2022). High-  
560 dimensional profiling reveals Tc17 cell enrichment in active Crohn’s disease and  
561 identifies a potentially targetable signature. *Nature Communications*, 13(1), Article 1.  
562 <https://doi.org/10.1038/s41467-022-31229-z>

563 Grumelli, S., Corry, D. B., Song, L.-Z., Song, L., Green, L., Huh, J., Hacken, J., Espada, R., Bag,  
564 R., Lewis, D. E., & Kheradmand, F. (2004). An Immune Basis for Lung Parenchymal  
565 Destruction in Chronic Obstructive Pulmonary Disease and Emphysema. *PLOS*  
566 *Medicine*, 1(1), e8. <https://doi.org/10.1371/journal.pmed.0010008>

567 Guan, H., Fan, D., Mrelashvili, D., Hao, H., Singh, N. P., Singh, U. P., Nagarkatti, P. S., &  
568 Nagarkatti, M. (2013). MicroRNA let-7e is associated with the pathogenesis of  
569 experimental autoimmune encephalomyelitis. *European Journal of Immunology*, 43(1),  
570 104–114. <https://doi.org/10.1002/eji.201242702>

- 571 Hamada, H., Garcia-Hernandez, M. de la L., Reome, J. B., Misra, S. K., Strutt, T. M.,  
572 McKinstry, K. K., Cooper, A. M., Swain, S. L., & Dutton, R. W. (2009). Tc17, a Unique  
573 Subset of CD8 T Cells That Can Protect against Lethal Influenza Challenge1. *The*  
574 *Journal of Immunology*, 182(6), 3469–3481. <https://doi.org/10.4049/jimmunol.0801814>
- 575 Hewitt, R., Farne, H., Ritchie, A., Luke, E., Johnston, S. L., & Mallia, P. (2016). The role of  
576 viral infections in exacerbations of chronic obstructive pulmonary disease and asthma.  
577 *Therapeutic Advances in Respiratory Disease*, 10(2), 158–174.  
578 <https://doi.org/10.1177/1753465815618113>
- 579 Hoenderdos, K., & Condliffe, A. (2013). The Neutrophil in Chronic Obstructive Pulmonary  
580 Disease. Too Little, Too Late or Too Much, Too Soon? *American Journal of Respiratory*  
581 *Cell and Molecular Biology*, 48(5), 531–539. <https://doi.org/10.1165/rcmb.2012-0492TR>
- 582 Huber, M., Heink, S., Pagenstecher, A., Reinhard, K., Ritter, J., Visekruna, A., Guralnik, A.,  
583 Bollig, N., Jeltsch, K., Heinemann, C., Wittmann, E., Buch, T., Costa, O. P. da, Brüstle,  
584 A., Brenner, D., Mak, T. W., Mittrücker, H.-W., Tackenberg, B., Kamradt, T., & Lohoff,  
585 M. (2013). IL-17A secretion by CD8<sup>+</sup> T cells supports Th17-mediated autoimmune  
586 encephalomyelitis. *The Journal of Clinical Investigation*, 123(1), 247–260.  
587 <https://doi.org/10.1172/JCI63681>
- 588 Ivanov, I. I., McKenzie, B. S., Zhou, L., Tadokoro, C. E., Lepelley, A., Lafaille, J. J., Cua, D. J.,  
589 & Littman, D. R. (2006). The orphan nuclear receptor ROR $\gamma$  directs the  
590 differentiation program of proinflammatory IL-17<sup>+</sup> T helper cells. *Cell*, 126(6), 1121–  
591 1133. <https://doi.org/10.1016/j.cell.2006.07.035>



- 592 Ivanov, I. I., Zhou, L., & Littman, D. R. (2007). Transcriptional Regulation of Th17 Cell  
593 Differentiation. *Seminars in Immunology*, *19*(6), 409–417.  
594 <https://doi.org/10.1016/j.smim.2007.10.011>
- 595 Izzotti, A., Calin, G. A., Arrigo, P., Steele, V. E., Croce, C. M., & De Flora, S. (2009).  
596 Downregulation of microRNA expression in the lungs of rats exposed to cigarette smoke.  
597 *The FASEB Journal*, *23*(3), 806–812. <https://doi.org/10.1096/fj.08-121384>
- 598 Jiang, S., Yan, W., Wang, S. E., & Baltimore, D. (2018). Let-7 Suppresses B Cell Activation  
599 through Restricting the Availability of Necessary Nutrients. *Cell Metabolism*, *27*(2), 393-  
600 403.e4. <https://doi.org/10.1016/j.cmet.2017.12.007>
- 601 Jin, Y., Wan, Y., Chen, G., Chen, L., Zhang, M.-Q., Deng, L., Zhang, J.-C., Xiong, X.-Z., & Xin,  
602 J.-B. (2014). Treg/IL-17 Ratio and Treg Differentiation in Patients with COPD. *PLOS*  
603 *ONE*, *9*(10), e111044. <https://doi.org/10.1371/journal.pone.0111044>
- 604 Kheradmand, F., Shan, M., Xu, C., & Corry, D. B. (2012). Autoimmunity in chronic obstructive  
605 pulmonary disease: Clinical and experimental evidence. *Expert Review of Clinical*  
606 *Immunology*, *8*(3), 285–292. <https://doi.org/10.1586/eci.12.7>
- 607 Kim, W. J., Lim, J. H., Lee, J. S., Lee, S.-D., Kim, J. H., & Oh, Y.-M. (2015). Comprehensive  
608 Analysis of Transcriptome Sequencing Data in the Lung Tissues of COPD Subjects.  
609 *International Journal of Genomics*, *2015*, 206937. <https://doi.org/10.1155/2015/206937>
- 610 Laniado-Laborín, R. (2009). Smoking and Chronic Obstructive Pulmonary Disease (COPD).  
611 Parallel Epidemics of the 21st Century. *International Journal of Environmental Research*  
612 *and Public Health*, *6*(1), Article 1. <https://doi.org/10.3390/ijerph6010209>
- 613 Lee, P. P., Fitzpatrick, D. R., Beard, C., Jessup, H. K., Lehar, S., Makar, K. W., Pérez-Melgosa,  
614 M., Sweetser, M. T., Schlissel, M. S., Nguyen, S., Cherry, S. R., Tsai, J. H., Tucker, S.

615 M., Weaver, W. M., Kelso, A., Jaenisch, R., & Wilson, C. B. (2001). A Critical Role for  
616 Dnmt1 and DNA Methylation in T Cell Development, Function, and Survival. *Immunity*,  
617 *15*(5), 763–774. [https://doi.org/10.1016/S1074-7613\(01\)00227-8](https://doi.org/10.1016/S1074-7613(01)00227-8)

618 Lee, S.-H., Goswami, S., Grudo, A., Song, L.-Z., Bandi, V., Goodnight-White, S., Green, L.,  
619 Hacken-Bitar, J., Huh, J., Bakaeen, F., Coxson, H. O., Cogswell, S., Storness-Bliss, C.,  
620 Corry, D. B., & Kheradmand, F. (2007). Antielastin autoimmunity in tobacco smoking-  
621 induced emphysema. *Nature Medicine*, *13*(5), 567–569. <https://doi.org/10.1038/nm1583>

622 Li, H., Liu, Q., Jiang, Y., Zhang, Y., Xiao, W., & Zhang, Y. (2015). Disruption of Th17/Treg  
623 Balance in the Sputum of Patients With Chronic Obstructive Pulmonary Disease. *The*  
624 *American Journal of the Medical Sciences*, *349*(5), 392–397.  
625 <https://doi.org/10.1097/MAJ.0000000000000447>

626 Lu, W., You, R., Yuan, X., Yang, T., Samuel, E. L. G., Marcano, D. C., Sikkema, W. K. A.,  
627 Tour, J. M., Rodriguez, A., Kheradmand, F., & Corry, D. B. (2015). MicroRNA-22  
628 Inhibits Histone Deacetylase 4 to Promote T Helper-17 Cell-Dependent Emphysema.  
629 *Nature Immunology*, *16*(11), 1185–1194. <https://doi.org/10.1038/ni.3292>

630 Mai, J., Virtue, A., Maley, E., Tran, T., Yin, Y., Meng, S., Pansuria, M., Jiang, X., Wang, H., &  
631 Yang, X.-F. (2012). MicroRNAs and other mechanisms regulate interleukin-17 cytokines  
632 and receptors. *Frontiers in Bioscience (Elite Edition)*, *4*, 1478–1495.

633 Morales-Mantilla, D. E., Huang, X., Erice, P., Porter, P., Zhang, Y., Figueroa, M., Chandra, J.,  
634 King, K. Y., Kheradmand, F., & Rodríguez, A. (2020). Cigarette Smoke Exposure in  
635 Mice using a Whole-Body Inhalation System. *JoVE (Journal of Visualized Experiments)*,  
636 *164*, e61793. <https://doi.org/10.3791/61793>

- 637 Newcomb, D. C., Cephus, J. Y., Boswell, M. G., Fahrenholz, J. M., Langley, E. W., Feldman, A.  
638 S., Zhou, W., Dulek, D. E., Goleniewska, K., Woodward, K. B., Sevin, C. M., Hamilton,  
639 R. G., Kolls, J. K., & Peebles, R. S. (2015). Estrogen and progesterone decrease let-7f  
640 microRNA expression and increase IL-23/IL-23 receptor signaling and IL-17A  
641 production in patients with severe asthma. *Journal of Allergy and Clinical Immunology*,  
642 *136*(4), 1025-1034.e11. <https://doi.org/10.1016/j.jaci.2015.05.046>
- 643 Pauwels, R. A., Buist, A. S., Calverley, P. M. A., Jenkins, C. R., & Hurd, S. S. (2001). Global  
644 Strategy for the Diagnosis, Management, and Prevention of Chronic Obstructive  
645 Pulmonary Disease. *American Journal of Respiratory and Critical Care Medicine*,  
646 *163*(5), 1256–1276. <https://doi.org/10.1164/ajrccm.163.5.2101039>
- 647 Peleman, R. A., Rytala, P. H., Kips, J. C., Joos, G. F., & Pauwels, R. A. (1999). The cellular  
648 composition of induced sputum in chronic obstructive pulmonary disease. *European*  
649 *Respiratory Journal*, *13*(4), 839–843. <https://doi.org/10.1034/j.1399-3003.1999.13d24.x>
- 650 Pottelberge, G. R. V., Mestdagh, P., Bracke, K. R., Thas, O., Durme, Y. M. T. A. van, Joos, G.  
651 F., Vandesompele, J., & Brusselle, G. G. (2011). MicroRNA Expression in Induced  
652 Sputum of Smokers and Patients with Chronic Obstructive Pulmonary Disease. *American*  
653 *Journal of Respiratory and Critical Care Medicine*, *183*(7), 898–906.  
654 <https://doi.org/10.1164/rccm.201002-0304OC>
- 655 Prevalence and attributable health burden of chronic respiratory diseases, 1990–2017: A  
656 systematic analysis for the Global Burden of Disease Study 2017. (2020). *The Lancet*.  
657 *Respiratory Medicine*, *8*(6), 585–596. [https://doi.org/10.1016/S2213-2600\(20\)30105-3](https://doi.org/10.1016/S2213-2600(20)30105-3)

- 658 Rodriguez, A., Griffiths-Jones, S., Ashurst, J. L., & Bradley, A. (2004). Identification of  
659 Mammalian microRNA Host Genes and Transcription Units. *Genome Research*, *14*(10a),  
660 1902–1910. <https://doi.org/10.1101/gr.2722704>
- 661 Schembri, F., Sridhar, S., Perdomo, C., Gustafson, A. M., Zhang, X., Ergun, A., Lu, J., Liu, G.,  
662 Zhang, X., Bowers, J., Vaziri, C., Ott, K., Sensinger, K., Collins, J. J., Brody, J. S., Getts,  
663 R., Lenburg, M. E., & Spira, A. (2009). MicroRNAs as modulators of smoking-induced  
664 gene expression changes in human airway epithelium. *Proceedings of the National*  
665 *Academy of Sciences*, *106*(7), 2319–2324. <https://doi.org/10.1073/pnas.0806383106>
- 666 Senior, R. M., & Anthonisen, N. R. (1998). Chronic Obstructive Pulmonary Disease (COPD).  
667 *American Journal of Respiratory and Critical Care Medicine*, *157*(4), S139–S147.  
668 <https://doi.org/10.1164/ajrccm.157.4.nhlbi-12>
- 669 Shan, M., Cheng, H.-F., Song, L., Roberts, L., Green, L., Hacken-Bitar, J., Huh, J., Bakaeen, F.,  
670 Coxson, H. O., Storness-Bliss, C., Ramchandani, M., Lee, S.-H., Corry, D. B., &  
671 Kheradmand, F. (2009). Lung Myeloid Dendritic Cells Coordinately Induce TH1 and  
672 TH17 Responses in Human Emphysema. *Science Translational Medicine*, *1*(4), 4ra10-  
673 4ra10. <https://doi.org/10.1126/scitranslmed.3000154>
- 674 Shan, M., You, R., Yuan, X., Frazier, M. V., Porter, P., Seryshev, A., Hong, J.-S., Song, L.,  
675 Zhang, Y., Hilsenbeck, S., Whitehead, L., Zarinkamar, N., Perusich, S., Corry, D. B., &  
676 Kheradmand, F. (2014). Agonistic induction of PPAR $\gamma$  reverses cigarette smoke-induced  
677 emphysema. *The Journal of Clinical Investigation*, *124*(3), 1371–1381.  
678 <https://doi.org/10.1172/JCI70587>
- 679 Shan, M., Yuan, X., Song, L., Roberts, L., Zarinkamar, N., Seryshev, A., Zhang, Y., Hilsenbeck,  
680 S., Chang, S.-H., Dong, C., Corry, D. B., & Kheradmand, F. (2012). Cigarette Smoke

681 Induction of Osteopontin (SPP1) Mediates TH17 Inflammation in Human and  
682 Experimental Emphysema. *Science Translational Medicine*, 4(117), 117ra9-117ra9.  
683 <https://doi.org/10.1126/scitranslmed.3003041>

684 Shi, J., & Petrie, H. T. (2012). Activation Kinetics and Off-Target Effects of Thymus-Initiated  
685 Cre Transgenes. *PLoS ONE*, 7(10), e46590. <https://doi.org/10.1371/journal.pone.0046590>

686 Veldhoen, M. (2017). Interleukin 17 is a chief orchestrator of immunity. *Nature Immunology*,  
687 18(6), Article 6. <https://doi.org/10.1038/ni.3742>

688 Wedzicha, J. A. (2004). Role of Viruses in Exacerbations of Chronic Obstructive Pulmonary  
689 Disease. *Proceedings of the American Thoracic Society*, 1(2), 115–120.  
690 <https://doi.org/10.1513/pats.2306030>

691 Williams, M., Todd, I., & Fairclough, L. C. (2021). The role of CD8 + T lymphocytes in chronic  
692 obstructive pulmonary disease: A systematic review. *Inflammation Research*, 70(1), 11–  
693 18. <https://doi.org/10.1007/s00011-020-01408-z>

694 Xu, C., Hesselbacher, S., Tsai, C.-L., Shan, M., Spitz, M., Scheurer, M., Roberts, L., Perusich,  
695 S., Zarinkamar, N., Coxson, H., Krowchuk, N., Corry, D., & Kheradmand, F. (2012).  
696 Autoreactive T Cells in Human Smokers is Predictive of Clinical Outcome. *Frontiers in*  
697 *Immunology*, 3. <https://www.frontiersin.org/articles/10.3389/fimmu.2012.00267>

698 Yeh, N., Glosson, N. L., Wang, N., Guindon, L., McKinley, C., Hamada, H., Li, Q., Dutton, R.  
699 W., Shrikant, P., Zhou, B., Brutkiewicz, R. R., Blum, J. S., & Kaplan, M. H. (2010).  
700 Tc17 Cells Are Capable of Mediating Immunity to Vaccinia Virus by Acquisition of a  
701 Cytotoxic Phenotype. *The Journal of Immunology*, 185(4), 2089–2098.  
702 <https://doi.org/10.4049/jimmunol.1000818>

703 You, R., Lu, W., Shan, M., Berlin, J. M., Samuel, E. L., Marcano, D. C., Sun, Z., Sikkema, W.  
704 K., Yuan, X., Song, L., Hendrix, A. Y., Tour, J. M., Corry, D. B., & Kheradmand, F.  
705 (2015). Nanoparticulate carbon black in cigarette smoke induces DNA cleavage and  
706 Th17-mediated emphysema. *eLife*, 4, e09623. <https://doi.org/10.7554/eLife.09623>

707 Zhang, H., Zhou, X., Chen, X., Lin, Y., Qiu, S., Zhao, Y., Tang, Q., Liang, Y., & Zhong, X.  
708 (2019). Rapamycin attenuates Tc1 and Tc17 cell responses in cigarette smoke-induced  
709 emphysema in mice. *Inflammation Research*, 68(11), 957–968.  
710 <https://doi.org/10.1007/s00011-019-01278-0>

711 Zhou, J.-S., Li, Z.-Y., Xu, X.-C., Zhao, Y., Wang, Y., Chen, H.-P., Zhang, M., Wu, Y.-F., Lai,  
712 T.-W., Di, C.-H., Dong, L.-L., Liu, J., Xuan, N.-X., Zhu, C., Wu, Y.-P., Huang, H.-Q.,  
713 Yan, F.-G., Hua, W., Wang, Y., ... Shen, H.-H. (2020). Cigarette smoke-initiated  
714 autoimmunity facilitates sensitisation to elastin-induced COPD-like pathologies in mice.  
715 *European Respiratory Journal*, 56(3). <https://doi.org/10.1183/13993003.00404-2020>

716 Zhu, H., Shyh-Chang, N., Segrè, A. V., Shinoda, G., Shah, S. P., Einhorn, W. S., Takeuchi, A.,  
717 Engreitz, J. M., Hagan, J. P., Kharas, M. G., Urbach, A., Thornton, J. E., Triboulet, R.,  
718 Gregory, R. I., Altshuler, D., & Daley, G. Q. (2011). The Lin28/let-7 Axis Regulates  
719 Glucose Metabolism. *Cell*, 147(1), 81–94. <https://doi.org/10.1016/j.cell.2011.08.033>

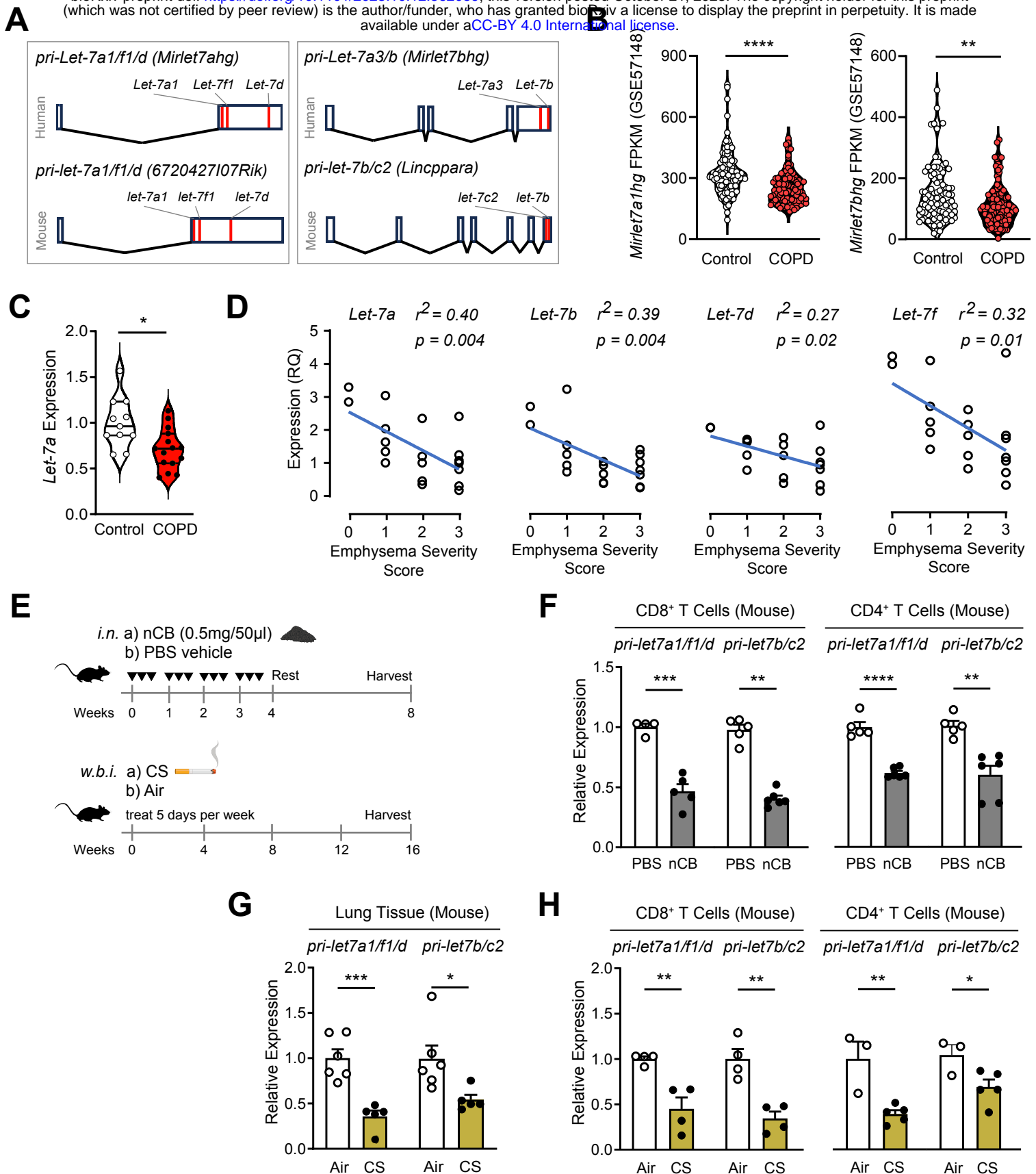


**Figure 1. Repression of *Let-7* miRNA gene clusters in lung T cells from COPD patients and murine models of emphysema.** (A) Schematic representation of the polycistronic transcripts for the *Let-7a1/Let-7f1/Let-7d*- and *Let-7b/Let-7a3*-clusters in humans and *let-7a1/let-7f1/let-7d*- and *let-7b/let-7c2*-clusters in mice. (B) *in silico* analysis of *Mirlet7a1hg* and *Mirlet7bhg* from the publicly available lung transcriptome dataset from RNA-seq of COPD and control patients (GEO: GSE57148). (C) Quantitative RT-PCR (qPCR) of mature *Hsa-Let-7a* from resected lung tissue of COPD (n=15) and control subjects (n=11). (D) qPCR and regression analysis of *Hsa-Let-7a*, *Hsa-Let-7b*, *Hsa-Let-7d*, and *Hsa-Let-7f* expression to emphysema severity score based on CT: 0=no, 1=upper lobes only, 2=upper/middle lobes, 3=extensive pan lobular emphysema (n=19). (E) Schematic diagram of experimental emphysema in mice induced by either intranasal (i.n.) instillation of nCB or exposure to CS by whole-body inhalation (w.b.i.). (F-H) qPCR analysis for *pri-let-7a1/f1/d* and *pri-let-7b/c2* from lung tissue or lung-derived CD8<sup>+</sup> and CD4<sup>+</sup> T cells of mice with emphysema elicited by (F) nCB- or (G-H) CS (n=3-6 per group). Data are representative of three independent experiments displayed as mean±SEM. Mann-Whitney (B,C) or Student's t-test (F,G,H). \*p < 0.05, \*\*p < 0.01, \*\*\*p < 0.001, \*\*\*\*p < 0.0001.

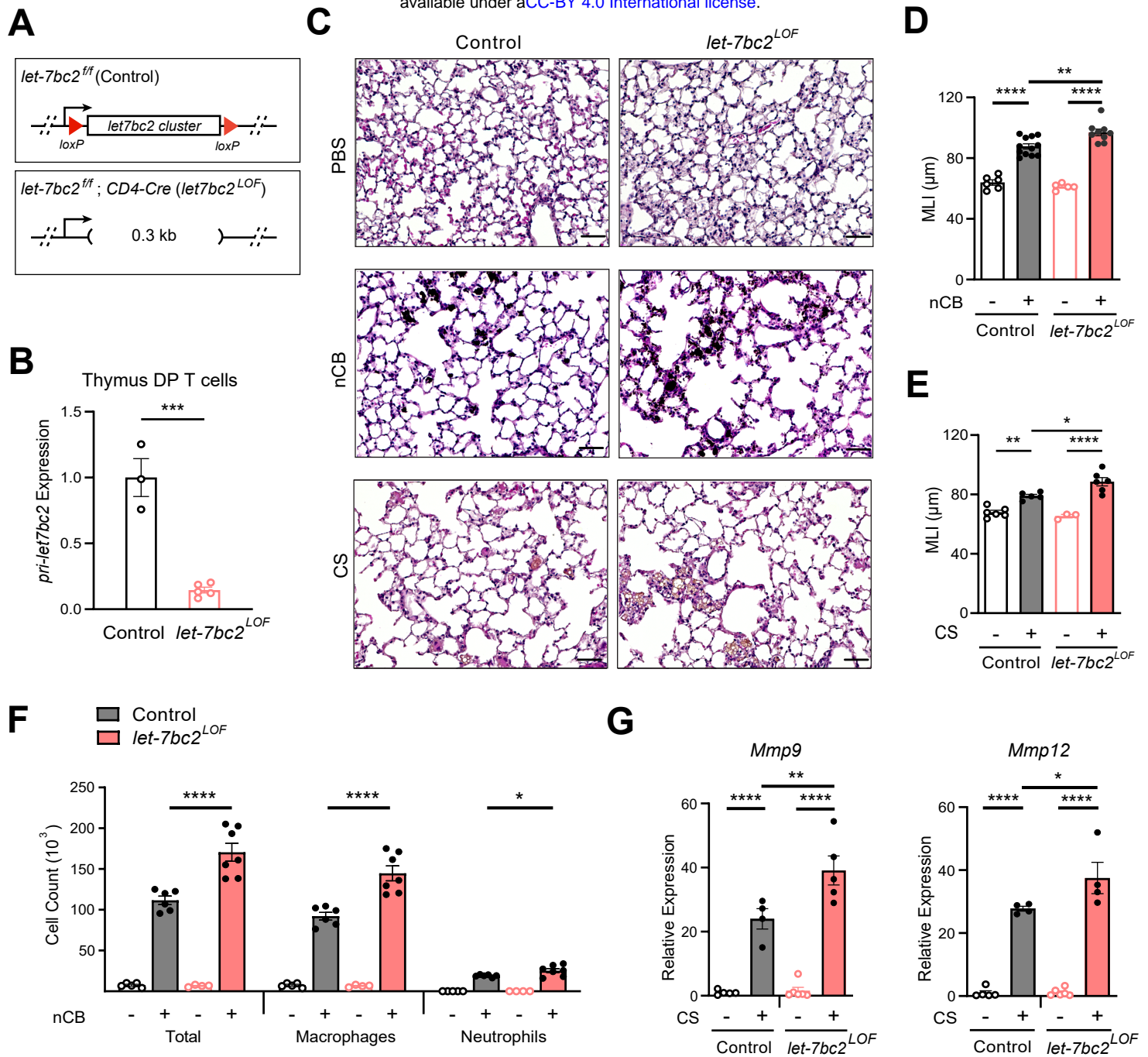


**Figure 2. Deletion of the *let7bc2* cluster in T cells enhances nCB- or CS-triggered emphysema.** (A) Schematic representation of CD4-Cre (*let7bc2*<sup>LOF</sup>) or *let7bc2*<sup>fl/fl</sup> (Control) mice. (B) qPCR analysis of pri-miRNA transcript for *pri-let7bc2* from flow-sorted live, TCRβ<sup>+</sup>, CD4<sup>+</sup>CD8<sup>+</sup> double-positive (DP) thymocytes of control and *let7bc2*<sup>LOF</sup> mice (n=3-5 per group). (C-G) Control and *let7bc2*<sup>LOF</sup> mice were exposed to vehicle (PBS) or nCB for 4 weeks, or alternatively air or cigarette smoke by whole body inhalation of cigarette smoke (CS) for 16 weeks. (C) Representative H&E stained lung sections from PBS-, nCB-, or CS-exposed mice as indicated on each panel (x20 magnification; scale bars, 50μm). (D-E) Mean linear intercept (MLI) measurement of lung morphometry. (F) Total and differential cell counts from bronchoalveolar lavage (BAL) fluid from controls and nCB-emphysemic mice (n=4-7 per group). (G) *Mmp9* and *Mmp12* mRNA expression from BAL cells of air- and smoke-exposed control and *let7bc2*<sup>LOF</sup> mice (n=4-6 per group). Data are representative of at least three independent experiments displayed as mean±SEM using Student's t-test (B) or two-way ANOVA with *post-hoc* Tukey correction (D,E,F,G). \*p < 0.05, \*\*p < 0.01, \*\*\*p < 0.001, \*\*\*\*p < 0.0001.



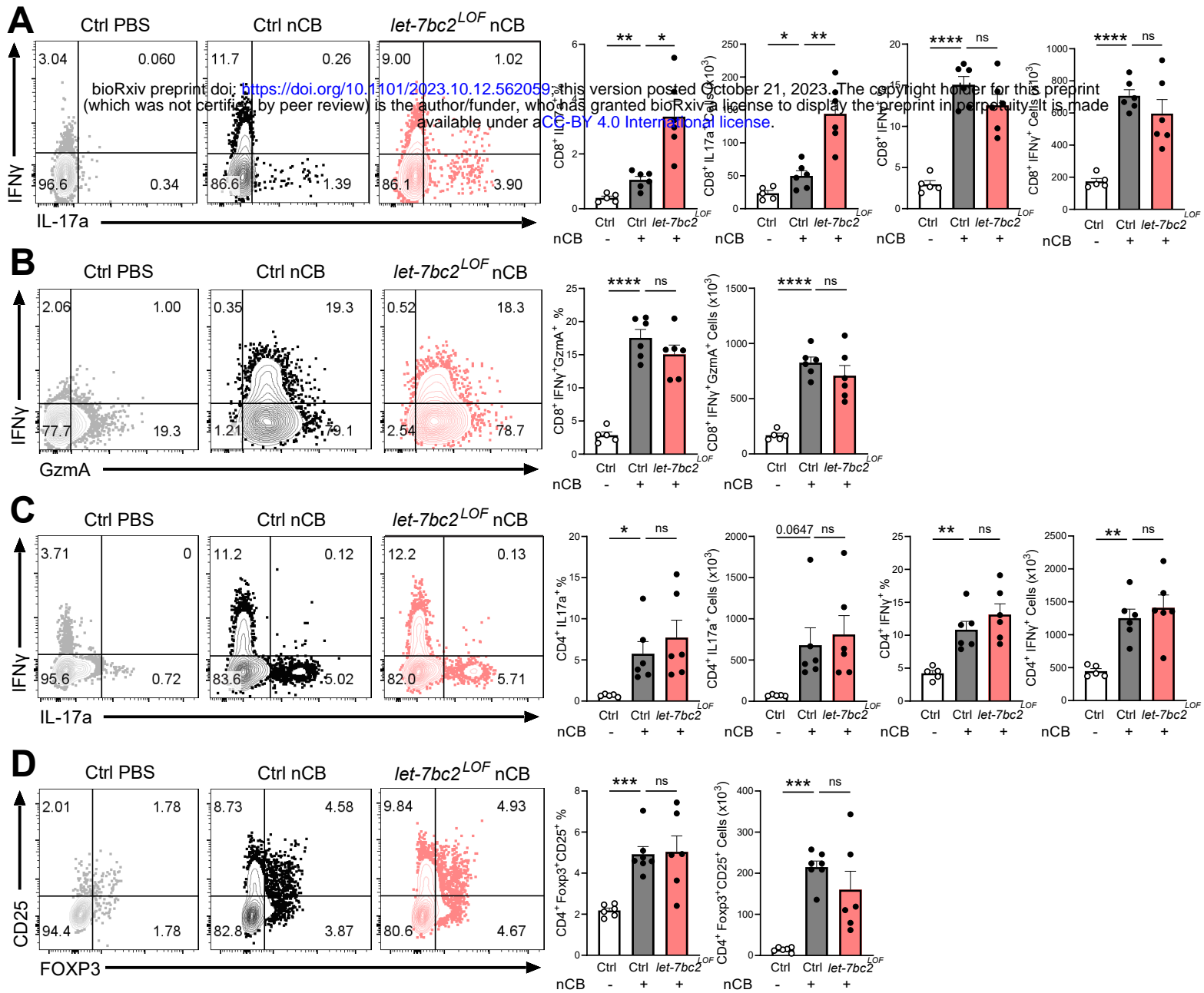


**Figure 3. *In vivo* T cell ablation of the *let-7bc2*-cluster enhances Tc17 inflammatory response to nCB-emphysema.** Representative flow plots with percentage and counts of live TCR $\beta^+$  (A) CD8 $^+$ IL-17a $^+$  and CD8 $^+$ IFN $\gamma^+$ , (B) CD8 $^+$ IFN $\gamma^+$ GzmA $^+$ , (C) CD4 $^+$ IL-17a $^+$  and CD4 $^+$ IFN $\gamma^+$ , and (D) CD4 $^+$  Foxp3 $^+$ CD25 $^+$  cells from the lungs of control PBS vehicle- (n=5-6), control nCB- (n=6), and *let-7bc2*<sup>LOF</sup> nCB-exposed mice. Data are representative of three independent experiments displayed as mean $\pm$ SEM using ANOVA with *post-hoc* Sidak correction. \*p < 0.05, \*\*p < 0.01, \*\*\*p < 0.001, \*\*\*\*p < 0.0001.

**A**

Rorc 3'UTR (mouse)

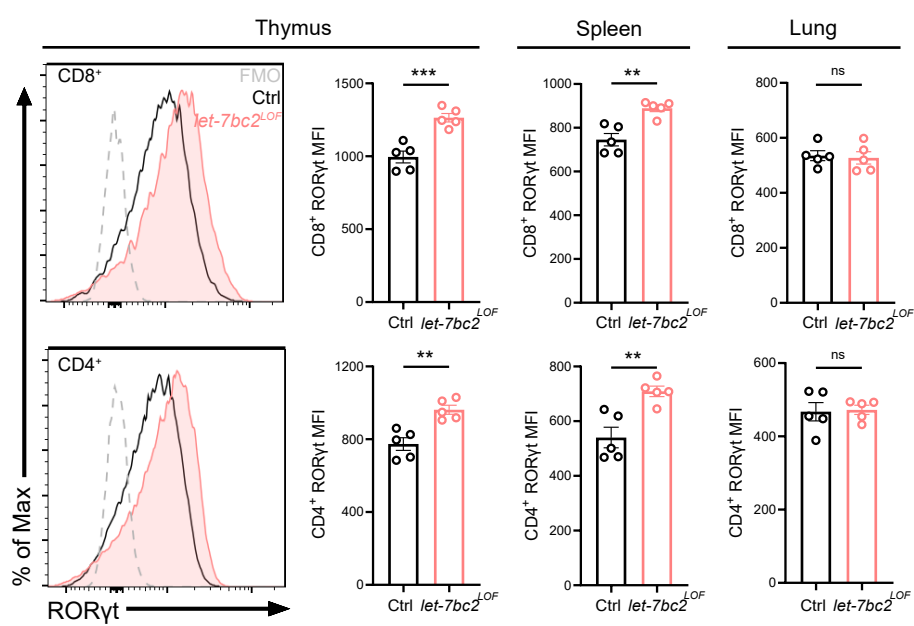
```

GCCAAGTGTGGAAAGCTGCAGATCTCCAGCAGCTCCACCCACCTGGTGTCCAGCCGCTCCCTCCACTCTATAAGGAAGCTTTCAGCACTGATGTTGAATCCCTGAGG
5' Q V E K L Q I F R H L H P I V V Q A A F P P L Y K E L F S T D V E S Y E
GGCTGTCAAGTGTATCTGGAGGAGGCAACTTCTATTTCCTCAGCCCTTGACCCGCTCCCTGGACTCCCTCCACCCAGCCTTCCCTTCTGCAGCTC
G L S K
TATGAAGGGTGTATCCCTAGGAGTAAGCAAACTCCTAAGACTGATTTTCTGCCCTAGGCTTGCTGTAGGACAACAGCAGCAAGTATGGAGAAAAGGCT
TGTATTGTTGATTTCCCAATAAGTTCACCCCTGGCTTGGAGAGCTGGGGTGAATGGATAGATAGAGTACCAAGTCAAAATAAAAAACAGACTGACA
7mer-A1
ATCAGAGGATAAAATCCAGTACTGGGATAAGGAGAACTCAATCTAGGCTGAAAGCTAATAACAGCTCTTCAATACCTCAATGTTATTTCCCTC
ATGGTCTCTCGGGGGGACATGGATCTAGCTCAGAGACTGGTGGCAAGCCCAAGAGACTGTATATAATAAGAAATAGATCTCTGAGACTTT
    
```

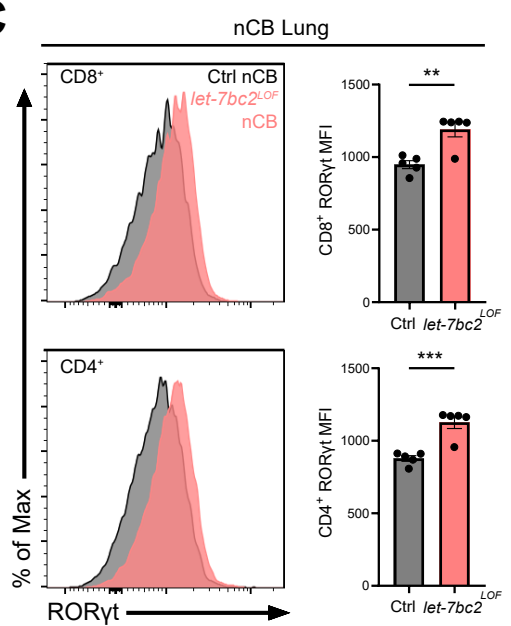
3' *let-7* UGAUGGAGU 5'

5' AAUACCUCAUU 3' mouse  
 5' AAUACCUCAUU 3' human  
 5' AAUACCUCAUU 3' cow  
 5' AAUACCUCAUU 3' dog  
 5' AAUACCUCAUU 3' elephant

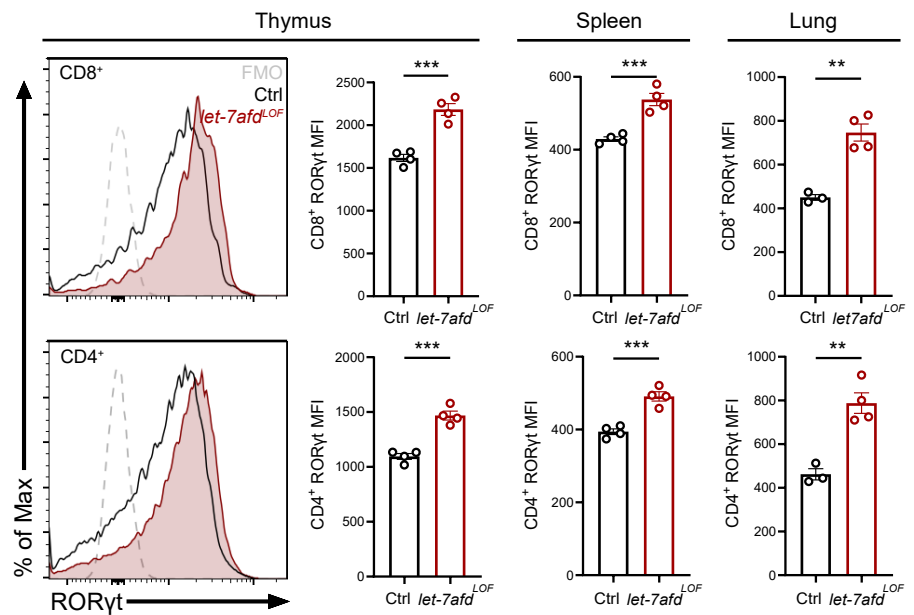
**B**



**C**



**D**



**E**

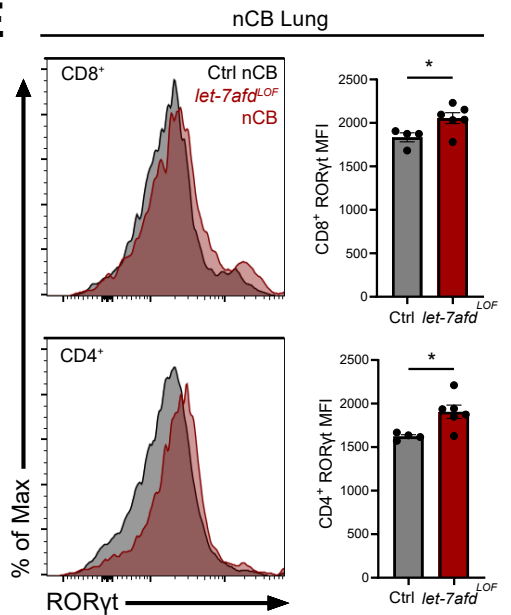


**Figure 4. Deletion of either the *let7bc2*- or *let7afd*-cluster in T cells enhances RORγt expression *in vivo*.** (A) Left: Schematic representation of the murine *Rorc* 3'UTR with *let-7* miRNA binding sites as identified by TargetScan. Right: Schematic of a conserved *let-7* miRNA target sequence in the 3'UTR of *Rorc*. (B-C) Flow analysis of RORγt expression by MFI quantification in live TCRβ<sup>+</sup>CD8<sup>+</sup> or CD4<sup>+</sup> T cells from indicated tissues of (B) naïve control and *let-7bc2*<sup>LOF</sup> mice or (C) nCB-treated lungs by representative flow plot and MFI quantification (n=5 per group). (D) RORγt expression by MFI quantification in naïve mice *let-7afd*<sup>LOF</sup> mice thymus, spleen, and lungs (n=3-4 per group), or (E) nCB-exposed lungs (n=5 per group). Data are representative of at least three independent experiments displayed as mean±SEM using student's t-test. \*p < 0.05, \*\*p < 0.01, \*\*\*p < 0.001, \*\*\*\*p < 0.0001.

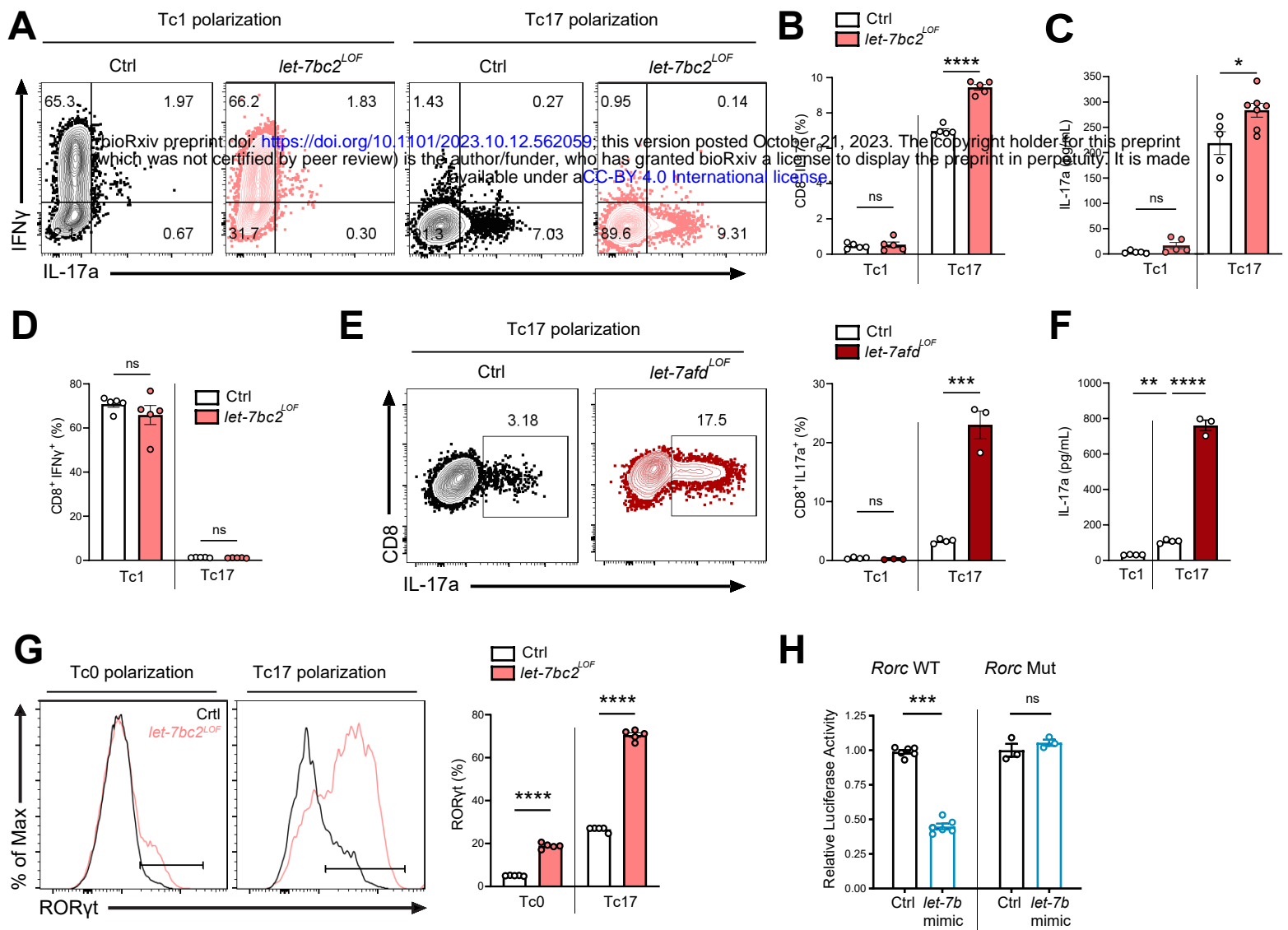


**Figure 5. *Let-7* restricts Tc17 *in vitro* differentiation in part via direct targeting of *Rorc* mRNA.** (A) Representative flow plots of live TCR $\beta$ <sup>+</sup> CD8<sup>+</sup>, IL-17a<sup>+</sup> and IFN $\gamma$ <sup>+</sup> populations from Tc1 and Tc17 polarized naïve splenic CD8<sup>+</sup> cells from control and *let-7bc2*<sup>LOF</sup> mice and (B) quantification of CD8<sup>+</sup>IL-17a<sup>+</sup> cells (n=5 per group). (C) ELISA of IL-17a from the supernatant of Tc1 and Tc17 polarized control and *let-7bc2*<sup>LOF</sup> cells (n=5-6 per group). (D) Flow quantification of CD8<sup>+</sup>IFN $\gamma$ <sup>+</sup> populations in Tc1 and Tc17 polarized control and *let-7bc2*<sup>LOF</sup> cells (n=5 per group). (E) Representative flow plots of CD8<sup>+</sup>IL-17a<sup>+</sup> population frequency in Tc17 polarized cells indicated mice, and (E) quantification of CD8<sup>+</sup>IL-17a<sup>+</sup> cells from control and *let-7afd*<sup>LOF</sup> mice polarized under Tc1 or Tc17 conditions. (F) ELISA of IL-17a from control Tc1 (n=4), control Tc17 (n=4), and *let-7afd*<sup>LOF</sup> Tc17 (n=3) polarized cells. (G) Representative flow plot and quantification of ROR $\gamma$ t from Tc0 or Tc17 differentiated naïve splenic CD8<sup>+</sup> T cells isolated from control and *let-7bc2*<sup>LOF</sup> mice (n=5 per group). (H) Control (*Rorc* WT) or binding site mutant (*Rorc* Mut) 3' UTRs of *Rorc* were cloned downstream of the renilla luciferase reporter. Plasmids were cotransfected with either a control-miR (black bars) or *let-7b* mimic (blue bars) duplex into cultured cells. Reporter activity was measured 24 hours after transfection and normalized to firefly activity. Data are representative of three independent experiments (A-G) or carried out in triplicate (H) and displayed as mean $\pm$ SEM using student's t-test. \*p < 0.05, \*\*p < 0.01, \*\*\*p < 0.001, \*\*\*\*p < 0.0001.

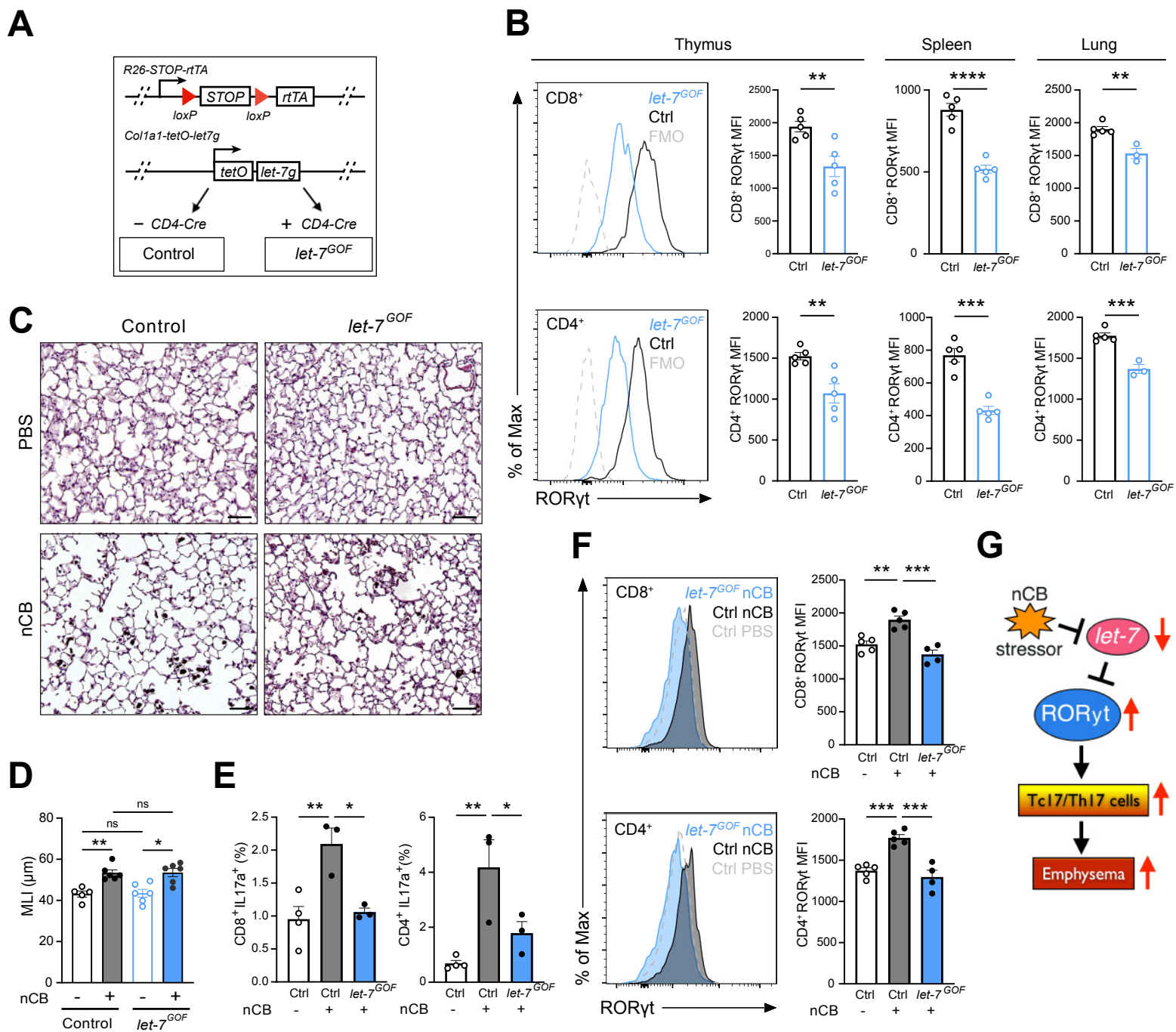


**Figure 6. Enforced *let-7* expression in T cells restrains induction of RORyt and Tc17/Th17 inflammation in lungs of nCB-exposed mice.** (A) Schematic outlining our T cell-inducible *let-7g* mouse model (*let-7<sup>GOF</sup>*). (B) Flow analysis of RORyt expression in live, TCRβ<sup>+</sup>CD8<sup>+</sup> or CD4<sup>+</sup> T cells from (B) naïve control and *let-7<sup>GOF</sup>* mice in thymus, spleen, and lungs (n=3-5 per group). (C) Control and *let-7<sup>GOF</sup>* mice were treated with PBS vehicle or nCB then analyzed. Representative H&E-stained lung sections from PBS- and nCB-exposed mice as indicated on each panel (x20 magnification; scale bars, 50μm) (D) MLI measurements from indicated mice (n=5-6 per group). (E) Flow analysis of lungs gated on live TCRβ<sup>+</sup> CD8<sup>+</sup> or CD4<sup>+</sup> cells for (E) IL-17a<sup>+</sup> population frequency (n=3-4 per group) or (F) RORyt expression by representative flow plot and MFI quantification (n=4-5 per group). (G) Figure model for *let-7*/RORyt axis in emphysema pathogenesis. Data are representative of two or three independent experiments and displayed as mean±SEM using student's t-test (B) or two-way ANOVA with Tukey's multiple correction (C,D,E). \*p < 0.05, \*\*p < 0.01, \*\*\*p < 0.001, \*\*\*\*p < 0.0001.